الجمهورية الجزائرية الديمقراطية الشعبية
PEOPLE'S DEMOCRATIC REPUBLIC OF ALGERIA
وزارة التعليم العالي والبحث العلمي
MINISTRY OF HIGHER EDUCATION AND SCIENTIFIC RESEARCH
جامعة سعد دحلب البليدة1
UNIVERSITY OF SAAD DAHLEB BLIDA 1

كلية العلوم
Faculty of Science
دائرة الفيزياء
Department of Physics

MASTER DIPLOMA THESIS
In Physics
Branch: Nanophysics

THEME

STUDY OF THERMO-RESISTIVE PROPERTIES OF METAL OXIDES THIN FILMS FOR THERMAL SENSORS

Presented by:

Mrs. Ghania CHOURAR - Mrs. Roufaida BEKHTI

Presented on 20/10/2021 in front of members of jury:

Dr. R. BELKADA	Research Director	CRTSE	President
Dr. A. Hassein-Bey	MCB	USDB	Examiner
Dr. Y. Khereddine	MRA	CDTA	Supervisor
Dr. S. Lafane	MRB	CDTA	Co-Supervisor

2020 / 2021

Acknowledgments

At first, we thank the Almighty Allah for giving us the strength, the will and the patience to complete this work.

To our parents,

We thank our dear parents, who have always been very close to us, thank you for the love that you give us, the care and the patience that you give us and for all what we need just to support us in our life. Actually words not enough to describe what **our parents** means to us life.

The presus work was carried out at the Center de development of advanced technologies in Algeriers (CDTA).

First , we would like to thank **Dr. Slimane LAFANE**, It is a great honor for us to see you sit on our jury. Your dedication to a job well done is the object of our consideration. Your professional background, your undeniable competence, your charisma and your human qualities make you a great teacher and we inspire great admiration and respect. Your kindness, your dynamism, your dedication to work and your competence aroused our admiration. We take this opportunity to express our gratitude to you for the time you spent with us this job. We pray, to accept our deep gratitude and our high consideration. You have done us the great honor of agreeing to lead us in this work with kindness and rigor. And all what you done for us cannot be in word.

Secondly, we would be more than glad to thank our advisor **MR. Khiradine YAZID.**

We acknowledge warmly ionized medium & laser division especially the Laser matter interaction group also Microelectronics & Nanotechnology Division of the CDTA for the easiness and the good progress of work. The authors would like to thank **Mr.Nait Bouda Lamine**, we thank you for your kindness and your precious help. **Mr. Smail LAFANE**, thank you for your precious help and advices. Thank you for all the knowledge you share with us.

To our Master, Option manager “Nanophysics” **Dr.Abdelkader Hassein-Bey**

It is a great honor for us to see you sit on our jury. We have had the great pleasure of working under your guidance, and we found with you the advisor and the guide who received us in all circumstances with sympathy, smile and kindness. You are a man of science and an attentive teacher, your incontestable professional competence as well as your human qualities you worth everyone's admiration and respect. You are and you will be for us the example of rigor and righteousness in the practice of the profession. We have found memories of the quality of teaching that you have lavished on us.

We would address our acknowledgements to the members of the jury, starting with the president of the jury **“Prof.R.BELKADA”**, the examiner **“Dr. Abdelkader Hassein-Bey”**, and the advisors **“Dr. S. Lafane”** and **“ Dr.Y. KHIRADINE”**, for giving us the honor to examine this work, and for the time and efforts that they have taken to read and correct this manuscript. We will certainly not forget all the teachers that taught us through all these academic years.

At last not least, it is more than a pleasure to address our acknowledgement to our family members, friends and every person that gave us material and emotional support, just to push us to study and reach this level.

Dedicate

TO MY VERY DEAR FAMILY,

To the sweet and most wonderful of all moms my MOM. To the one who helped me discover "knowledge" the inexhaustible treasure DAD. The fruit of your countless sacrifices, though I never forgive you enough. May this modest work be the fulfillment of my family wish.

To my sisters ***Houda*** *and* ***Rania*** *and my only one brother* ***Islam Belkacem****, I will always pray to Allah for bliss you to me.*

Thank you ***my dear parents****, my soul for you MOM and DAD.*

To my friends from my childhood thank you for being a part of my life.

Bekhti Roufaida

TO MY VERY DEAR FAMILY,

To my all and the only one woman that I care about it MOM. To the one who helped me discover "knowledge" the inexhaustible treasure DAD.

To my sisters ***Meriem*** *and* ***Zahra*** *that was always with me and help me every time and make me feel that am not alone.*

To ***Loubaba***, ***Basma*** *and* ***Madjda*** *my dear friends thank you for being in my life and care about me from my childhood.*

Chourar Ghania

ملخص

حتى الآن، تم استخدام العديد من مواد الاستشعار الحراري لتطوير أجهزة الاستشعار الحرارية، بما في ذلك المعادن وأشباه الموصلات. من بين هذه الأخيرة، في هذه الدراسة، استخدمنا أكسيد الفناديوم وسمكات مختلفة من أكسيد الزنك بسبب خصائص مقاومتهم الحرارية الممتازة بما في ذلك المعامل العالي للمقاومة الحرارية.(TCR) في هذا السياق، أجرينا دراسة تستند إلى قياس TCRs لأغشية أكسيد الفناديوم واكسيد الزنك الرقيقة، وبالتالي تحديد الظروف التجريبية المثلى لتصنيع هذه الطبقات.

يُظهر التحليل الهيكلي باستخدام حيود الأشعة السينية (XRD) ومطياف رامان أن الأغشية الرقيقة من أكسيد الفاناديوم تحتوي على V_2O_5 كمرحلة رئيسية مع مرحلة ثانوية من V_6O_{13} . بينما تدل القياسات الكهربائية على وجود مرحلة VO_2. يوضح XRD أيضًا أن أغشية ZnO الرقيقة ذات جودة عالية وأن التبلور يعتمد على السماكة.

توضح القياسات الكهربائية لمقاومة الأغشية بطريقة 04 نقطة كدالة لدرجة الحرارة أن TCR لأغشية أكسيد الفاناديوم الرقيقة يعتمد على تيار التحيز ، على عكس ZnO. في درجة حرارة الغرفة (27 درجة مئوية) ، يكون TCR لأغشية أكسيد الفاناديوم الرقيقة 2.7٪ / درجة مئوية و 7٪ / درجة مئوية ، على التوالي , 1 و 10 µA ومقاومة كبيرة نسبيًا من 35 و 367Ωcm. TCR مرتفع حتى 30٪ / درجة مئوية عند 47 درجة مئوية المقابلة لدرجة حرارة انتقال العازل المعدني لمرحلة VO 2. على الجانب الآخر ، تُظهر الأغشية الرقيقة ZnO القليل جدًا من TCR بنسبة 0.06٪ / درجة مئوية لسمك 1200 نانومتر وقريب من الصفر TCR لسمك 500 و 100 نانومتر مع مقاومة في حدود 10-2 إلى 10-4 ميكرومتر. علاوة على ذلك ، لم يلاحظ أي حلقة تخلفية في أغشية ZnO الرقيقة. في الأغشية الرقيقة لأكسيد الفاناديوم ، يتم التحكم في حلقة التخلفية بواسطة درجة حرارة حدية تؤكد بدء الانتقال في VO_2 .

أخيرًا ووفقًا لنتائجنا ، تعتبر الطبقات النشطة من أكسيد الفاناديوم النانوية مرشحة واعدة لأجهزة الاستشعار الحرارية شديدة الحساسية ، في حين أن ZnO له أهمية كبيرة لتصميم مستشعرات الأغشية الرقيقة المقاومة للضغط.

Abstract

To date, a number of thermal sensing materials have been used to develop thermal sensors, including metals and semiconductors. Among this the latter, vanadium oxide and various thicknesses of zinc oxide are commonly used due to their excellent refractory properties including a high thermal resistance coefficient (TCR).

In this context, we propose a study based on TCRs measurement of vanadium oxide and zinc oxide thin films, so to determine the optimal experimental conditions for the fabrication of these layers.

The structural analysis using X-Ray diffraction (XRD) and Raman spectroscopy shows that vanadium oxide thin films contain V_2O_5 as a main phase with a secondary phase of V_6O_{13}. While the electrical measurements evidences the presence of a VO_2 phase. XRD shows also that ZnO thin films are of high quality and the crystallinity is thickness dependent.

The electrical measurements of films resistance by 04-point method as a function of temperature shows that TCR of vanadium oxide thin films depends on the bias current, contrary to ZnO. At room temperature (27°C), the TCR of Vanadium oxide thin films is 2.7 %/°C and 7% /°C, for respectively, 1 µA and 10 µA bias currents and relatively large resistivity of 35 and 367 Ωcm. The TCR is high up to 30%/°C at 47°C corresponding to the metal-insulator transition temperature of VO2 phase. On the other side, ZnO thin films shows a very little TCR of 0.06%/°C for 1200 nm thickness and near Zero TCR for 500 and 100 nm thicknesses with a resistivity in the range of 10-2 to 10-4 Ωcm. Further, no hysteresis loop is observed in ZnO thin films. In vanadium oxide thin films, the hysteresis loop is controlled by a threshold temperature that corroborates the initiation of the transition in VO_2 .

Finally and according to our results, vanadium oxide nanocomposite active layers are promising candidates for highly sensitive thermal sensors, whereas ZnO is of a great interest to design piezoresistive thin-film sensors.

Résumé

A ce jour, un certain nombre de matériaux de détection thermique ont été utilisés pour développer des capteurs thermiques, y compris des métaux et des semi-conducteurs. Parmi ces derniers, dans cette étude, nous avons utilisé l'oxyde de vanadium et plusieurs épaisseurs d'oxyde de zinc en raison de leurs excellentes propriétés thermo-résistives dont un coefficient de résistance thermique (TCR) élevé. Dans ce contexte, nous avons réalisé une étude basé sur la mesure du TCR des couches minces d'oxyde de vanadium et de situer par conséquence les conditions expérimentales optimales de fabrication de ces couches.

L'analyse structurale utilisant la diffraction des rayons X (DRX) et la spectroscopie Raman montre que les films minces d'oxyde de vanadium contiennent du V_2O_5 comme phase principale avec une phase secondaire de V_6O_{13} . Tandis que les mesures électriques mettent en évidence la présence d'une phase VO_2 . La DRX montre également que les films minces de ZnO sont de haute qualité et que la cristallinité dépend de l'épaisseur. Les mesures électriques de résistance des films par la méthode des 04 points en fonction de la température montrent que le TCR des films minces d'oxyde de vanadium dépend du courant de polarisation, contrairement au ZnO. A température ambiante (27°C), le TCR des films minces d'oxyde de vanadium est de 2,7%/°C et 7% /°C, pour respectivement, des courants de polarisation de 1 µA et 10 µA et une résistivité relativement importante de 35 et 367 Ωcm. Le TCR est élevé jusqu'à 30%/°C à 47°C correspondant à la température de transition métal-isolant de la phase VO2. D'un autre côté, les couches minces de ZnO présentent un très faible TCR de 0,06 %/°C pour une épaisseur de 1200 nm et un TCR proche de zéro pour des épaisseurs de 500 et 100 nm avec une résistivité comprise entre 10-2 et 10-4 Ωcm. En outre, aucune boucle d'hystérésis n'est observée dans les films minces de ZnO, tandis que dans les films minces d'oxyde de vanadium, la boucle d'hystérésis est contrôlée par une température seuil de chauffage en relation avec l'initiation de la transition isolant-métal du VO_2 .

Finalement et d'après nos résultats, les couches actives nanocomposites d'oxyde de vanadium sont des candidats prometteurs pour les capteurs thermiques hautement sensibles, tandis que le ZnO présente un grand intérêt pour la conception de capteurs piézorésistifs à couche mince.

List of contents

CHAPTER III : RESULTS AND DISCUSSIONS

List of figures

Chapter I

Chapter II

Chapter III

List of tables

Chapter III

Introduction

Thermal sensors are found in many items, from commonplace items inside any home to more sophisticated applications. It is vital for processors to stay within the temperature range specification to perform reliably and for the processor to run at its expected speed performance. The basic principle of thermal sensors is the thermo-resistive property. The development of thermal sensors is closely linked to the efficiency of thermal sensing materials. Were many materials have been used to develop thermal sensors but, metal oxides is the good candidate in this field due to its high temperature coefficient of resistance (TCR).

Several studies are being done to improve the sensitivity of thermal detection materials, in order to obtain very sensitive sensors, in this study we based on TCRs measurement of vanadium oxide and zinc oxide thin films deposited on glass substrates by pulsed laser deposition technique. The objective is to find proper parameters to get a high TCR, low resistivity and reversibility through the heating and the cooling cycle.

This work contains three chapters:

The first chapter gives basic theory of thermal sensors and the state of the art of vanadium oxides and zinc oxide thin films based sensors.

Chapter II reviews pulsed laser deposition of thin films technique, and the methods of characterization that are used in the present work. In depth, details about the experimental aspects pertaining to this thesis are provided in this chapter, whereas results and discussion are detailed in chapter III. Finally a conclusion is given.

Chapter I

Thermal Sensors

I.1 Introduction

Temperature is a key physical metric associated with different fields of science and technologies. It is generally linked with safety and performance used for important decision making in industries. In the semiconductor industry, thermal sensing and temperature measurement of a silicon device is considered a necessary step towards the qualification and certification of the applications device. Thermal sensors are found in many items, from commonplace items inside any home to more sophisticated applications. Can found sensors in household electronics like thermostats or thermometers. In personal computer or in a microprocessor. Several studies are being done to improve the sensitivity of thermal detection materials, in order to obtain very sensitive sensors with taking into account characteristics such as size, operating temperature range, response time, cost, lifetime, and energy consumption [8].

There are many types of thermal sensors that exist today, and each has a working principles. The principles of some of these sensors are described in the first part of this chapter. The development of thermal sensors is closely linked to the efficiency of thermal sensing materials, so the second part of the chapter describes two widely used metal oxides in the development of thermal sensors, which are studied in this work.

I.2 Backgrounds

I.2.1 Thermal sensors

MEMS (Micro Electro-Mechanical Systems) sensors have been developed aiming at high sensitivity, fast response, stability and reproducibility, miniaturization capability and mass production. The working principle of these sensors is based on a variety of physical phenomena such as thermoresistive, piezoresistive, pseudo hall, thermoelectric and piezoelectric effects [1, 2]. Among these effects, the thermoresistive effect, which refers to the electrical resistance change with temperature variation, has many advantages in terms of simplicity in design and implementation. Based on this effect, various micro-sized thermal sensors, which can monitor temperature [3], flow [4], [5] and acceleration [6, 7], have been successfully fabricated.

Temperature is the measure of the average kinetic energy of the molecules of a gas, liquid, or solid. A thermal sensor is a device that is specifically used to measure temperature. In this way, thermal sensors are able to give us a quantifiable way to describe the substance, whether it is an object, the environment in which an object is placed or the environment in which an object is distributed [8].

Many types of thermal sensors transduce a thermal signal directly into an electrical signal. Such types of sensors include thermocouples, thermistors, and transistors. Other types of thermal sensors convert a temperature change into mechanical deflection that can be transduced into an electrical signal [9]. In the following, the most common detection mechanisms will be discussed.

I.2.1.1 Detection mechanisms

a) Thermocouples: thermocouples are sensors composed of two different metals at their sensing end. A voltage is created when there is a temperature gradient between the hot sensor element and the cold reference junction. The change in voltage can be reported as a temperature through the Seebeck effect. The Seebeck effect says that the change in voltage is linearly proportional to the change in temperature and the two variables are related to each other through a coefficient that is determined by the materials used in the thermocouple. Fig I.1 depicts the construction of a thermocouple.

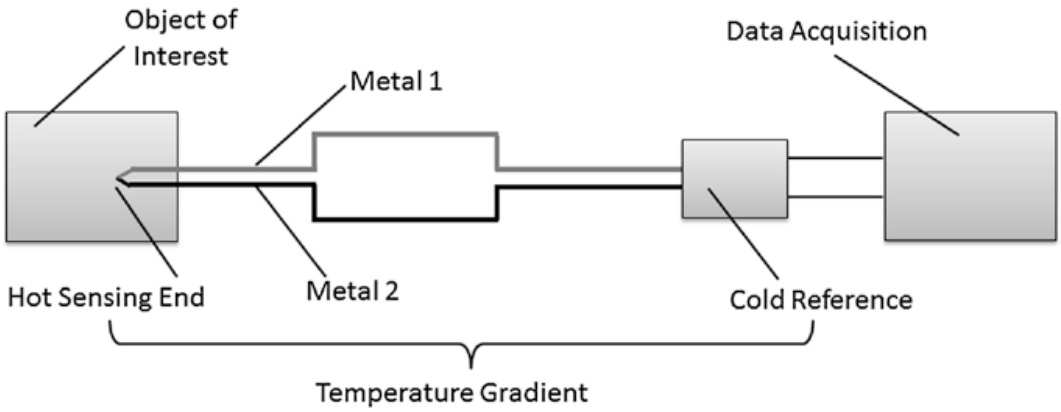

***Figure I.1**: Thermocouple construction* [8].

b) Resistance Thermometers and Thermistors: resistance thermometers are also known as resistance temperature detectors, or RTDs. They are typically made of a single pure metal. Each metal has a material property of electrical resistance that is a function of temperature. The most accurate resistance thermometers are ones that use metals that have a very linear relationship with temperature, such as platinum. By using the relationship curves between electrical resistance and temperature, when the resistance of the metal is measured, a temperature can be calculated. Fig I.2 depicts a type of resistance thermometer.

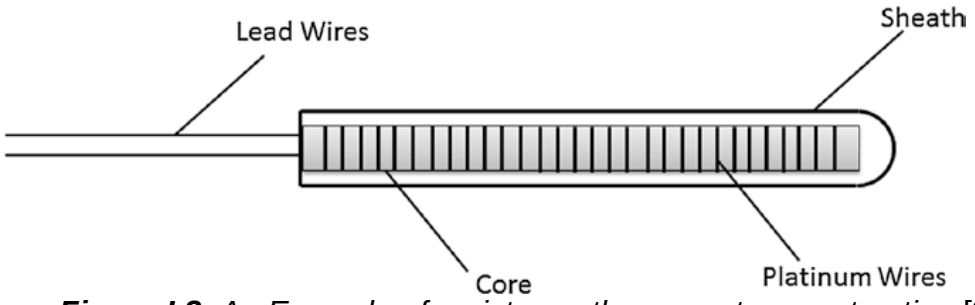

Figure I.2: *An Example of resistance thermometer construction* [8].

A thermistor is a specific type of resistance thermometer. Thermistors are made of metal wires connected to a ceramic base made of several sintered, oxide semiconductors. Unlike traditional resistance thermometers, the relationship is not very linear. Thus, the temperature range in which thermistors can be used is small compared to traditional resistance thermometers. But thermistors have the advantages of being small in size, inexpensive to buy and very sensitive to temperature changes, so they can be ideal to use in many electronics applications [8].

c) CMOS Temperature Sensors: CMOS (complementary metal-oxide-semiconductor) sensors are devices fabricated by the standard silicon microfabrication process. CMOS temperature sensors can be categorized as a special type of thermistor that uses silicon as the sensing material. Since the carrier concentration of silicon is dependent on the temperature, any type of electrical element integrated onto silicon including resistor, diode, and transistor can be potentially utilized as a temperature sensor. The temperature can be found by measuring the temperature-dependent voltage-current (V-I) characteristics. Most CMOS temperature sensors are bipolar

transistors because the base-emitter voltage and saturation current have good temperature characteristics. Temperature is determined by the signals generated from the base-emitter voltage and the saturation current. All the integration is done on the surface of a microchip, making it not only extremely portable but also mass producible [9].

d) Radiation Thermometers: All substances and objects emit thermal radiation when it is at a temperature higher than absolute zero (0 K or −273.15 °C). There is a relationship between temperature and radiation energy emitted that can be used to calculate the temperature of the object surface. Unlike other sensors discussed above, radiation thermometers are primarily used at a distance from the object of interest and can be used for hard-to-reach objects [8]. The Golay cell is one example of radiation thermometers. The Golay cell contains a blackened pneumatic chamber (like a balloon) with an illuminated flexible mirror on it. As gas in the chamber is heated by the incoming radiation, the chamber expands and a beam reflected by the mirror moves. That move changes the irradiance of another detector, and that signal is then processed. Another example of radiation thermometers is the bolometers and microbolometers. Infrared detection by bolometers and microbolometers depends on the change in electrical resistance of a material as the temperature of the material changes [10].

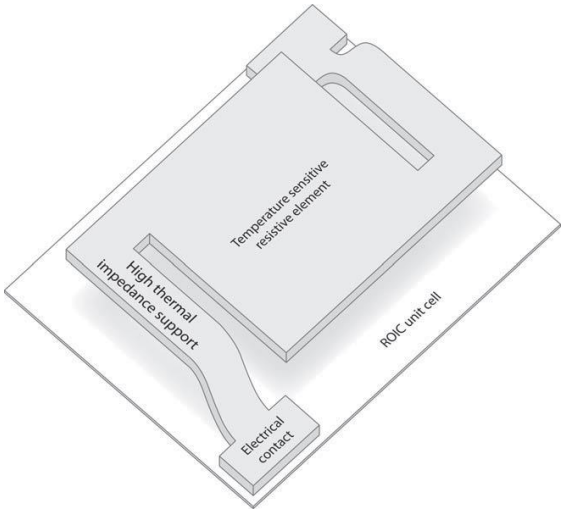

Figure I.3: *Microbolometer* [10].

e) Bilayer Cantilever Sensors: A bilayer cantilever consists of two layers of different materials. The temperature is found by measuring the deflection of the cantilever, which results from the different thermal expansion coefficients of the top film and the probe body (see Fig. I.4). If a piezoelectric material is a part of the bi-material cantilever, the deflection will result in a measurable voltage produced. These cantilevers are also useful in the application of actuators [9].

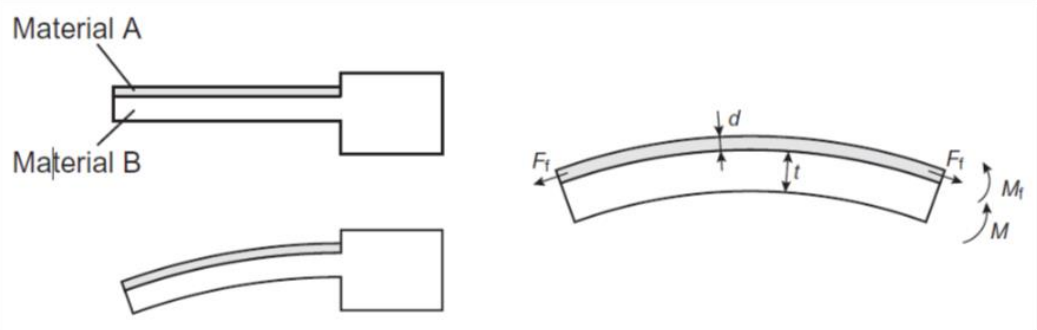

Figure I.4: *Schematic diagram of a bi-material cantilever sensor* [9].

I.2.1.2 Figures of merit

Each thermal sensor has a special detection mechanism; therefore competence is based on varieties of parameters for each sensor. The performance of the bolometer infrared detectors can be expressed in terms of responsivity (R_V), which represents the signal generated per unit incident power and it is expressed in ***equation I.1***

$$R_V = \frac{I_b R_\alpha \eta}{G\sqrt{1+\omega^2\tau^2}} \qquad (\text{I. } 1)$$

where I_b is the bias current; R the electrical resistance; α the temperature coefficient of resistance (TCR); η the absorptivity of the thin films; G the thermal conductance of the suspended structure; ω the modulation frequency set by the mechanical chopper; τ the thermal time constant equal to C/G, where C is the thermal mass of the isolated structure. From Eq. (I.1), it can be seen that the responsivity is high for high TCR values. Therefore, TCR is represents the merit that influences the performance of uncooled microbolometers and hence, it is the vital parameter to characterize the materials for IR sensing layer for thermal imaging application [11].

Thermistors are essentially resistors with a high temperature coefficient of resistance (TCR): given by the following ***equation I.2***

$$TCR = \frac{dR_T}{R_T dT} \quad (\mathrm{I}.2)$$

The thermistor resistance R_T changes exponentially with temperature T and can be described by the relationship:

$$R_T = R_0 e^{\frac{B}{T}} \quad (\mathrm{I}.3)$$

The B constant (beta factor or coefficient of thermal sensitivity) is a thermistor parameter, which reflects the change in resistance with temperature. The value of β constant can be determined based on the following formula:

$$B = \frac{T_1 T_2}{T_2 - T_1} \ln \frac{R_1}{R_2} \quad (\mathrm{I}.4)$$

where, R_1 and R_2 are resistances at temperatures T_1 and T_2 respectively [8].

Resistivity is one of the important parameters affect in the performance of a microbolometer. Low resistivity yields low thermal noise in addition to low power dissipation in the microbolometer. The low resistivity of the material allows it to be used in planar microbolometers and makes it easy to match them with readout electronics based on bipolar transistors, and makes it easier to read the pixels with the associated ROIC (readout integrated circuit).

I.2.2 Metal oxide thin films

Many materials can be used to develop thermal sensors, but metal oxides thin films is a good candidate for this field thanks to its high temperature coefficient of resistance (TCR). Metal oxides represent one of the important classes of functional materials in view of their abundance for their practical deployment and opportunities for value addition for continuous quality/performance improvement. In this work, focus is placed on the oxides of zinc and vanadium.

I.2.2.1 Vanadium oxide

Among the many candidate materials that have been investigated for use as microbolometer image sensors, including materials such as amorphous silicon, the most popular one is vanadium oxide (VO_x) due to its high TCR value, low noise, fast thermal time constants, good IR absorption and tunable electrical conductivity. A set of vanadium oxides, such as VO, V_2O_3, VO_2, and V_2O_5, exist due to the half d shell of the vanadium atom. Among these oxides, V_2O_5 is widely studied for its high temperature coefficient of resistivity (TCR) in a large temperature range.

In general, vanadium oxide is prepared using magnetron sputtering or pulsed laser deposition, and it has quite high TCR values in the range of about 2–3%/K with relatively low 1/*f* noise depending on the stoichiometry and the preparation of the film, proved quite sufficient for use in commercial microbolometers [12, 13]. It is possible to achieve high TCR values up to -7%/K under optimized deposition condition [14]. At room temperature, high TCR vanadium oxide thin film of 6.5%/K for microbolometer applications has been achieved by growing mixed phases of VO_2 and V_2O_3 with the method of reactive ion sputtering [15]. N.Fieldhouse deposited VO_x thin films with the TCRs in the range of -1.1% to -2.4%/K by reactive pulse direct current (dc) magnetron sputtering process [16]. C. Venkatasubramanian reported that low resistivity VO_x thin films with the TCRs in the range of -1.6% to -2.2%/K were deposited by pulsed-dc sputtering [17]. He also performed ion implantation followed by annealing to improve the trade-off between TCR and resistivity. The resistivities of the VO_x thin films ranged from 0.05 Ωcm to 100 Ωcm and the TCR values varied from -1.1% to -2.7% [18]. B. D. Gauntt increased the TCR to the value of -3.5%/°C by increasing oxygen content using pulsed dc magnetron sputtering in an atmosphere containing argon and oxygen [19].

I.2.2.2 Zinc oxide

Zinc Oxide (ZnO) is among the most important semiconductors used in the industry as a very sensor element. ZnO has attracted attention to be used as the active layer of the microbolometer detectors, due to its potential to have TCR values higher than that of the commercially used materials. Several research groups have obtained

results suggesting that ZnO indeed has higher TCR values than VO_x and a-Si. Zhou et al. used PLD technique for ZnO deposition, and they observed TCR values ranging from -3.4 to -13%K^{-1} [20]. Enes Battal et al investigate the application potential of atomic-layer-deposited ZnO in uncooled microbolometers, and reported that The temperature coefficient of resistance is observed to be as high as -10.4%K^{-1} near room temperature with the ZnO thin film grown at 120 °C [21]. Also doping of ZnO has been used to increase the TCR of ZnO, Zhou reported a TCR value of -17.5 % K^{-1} at 244 K for bolometers based on ZnO films doped with silver [22]. X.F. Zhou et al. [23] deposited Co-doped ZnO thin films by the pulsed laser deposition technique on Si (111) single-crystal substrates. With a low substrate temperature, a high TCR appeared in these Co-doped ZnO films. The largest TCR observed was as high as -20 % K^{-1} at a substrate temperature of 120 °C with a Co concentration of 10 %. Tuning of zinc oxide temperature sensing by tin heavy-doping reported by N. Al-Khalli et al. [24] , who revealed an increase in the visible and infrared radiation absorption and electrical conductivity with increasing Sn doping whereas the temperature coefficient of resistance (TCR) decreases. A maximum TCR value of 1.9%/K with a sheet resistance (R_s) of 233 kΩ/square was observed with 22% Sn doping concentration. The result proved that the Sn doping could help to decrease the TCR temperature dependence and the sheet-resistance of ZnO thin film as well as increasing its IR radiation absorption that makes it a strong candidate for the active layer of microbolometer. Measurements of thermo-electric parameters on self-assembled Ag/ZnO nanostructures (with the highest ZnO concentration) fabricated with seeds by John E. Sanchez et al. [25] showed high room temperature TCR values up to -11.8% K^{-1}, in addition the TCR and conductivity of the material can be tuned with the Ag/ZnO concentration ration.

Chapter II

Experimental procedure

II.1 Introduction

The deposition of thin layers, was carried out by different deposition techniques with different metal oxides, giving several electrical characteristics. This chapter will present the thermo-resistive effect by the experimental study of analysis of electrical properties.

II. Thin films deposition techniques

In electro-deposition scientists have developed many thin Film deposition techniques can be achieved through two methods: Physical Vapour Deposition (PVD) or Chemical Vapour Deposition (CVD) [26].

In this experiment we have used for the oxides metals physical vapour deposition (PVD), technique wich is one of the oldest methods of depositing metal films. as shown in ***Figure.II.2***

The technique of physical vapor deposition (PVD) is based on the vapor formation of the material to be deposited as a thin layer. It is fundamentally a vaporization coating process in which the basic mechanism is an atom by atom transfer of material from the solid phase to the vapor phase and back to the solid phase, gradually building a film on the surface to be coated. In the case of reactive deposition, the depositing material reacts with a gaseous environment of co-deposited material to form a film of compound material. The most useful depositions technique is pulsed laser deposition (PLD) and thermal evaporation (TE).

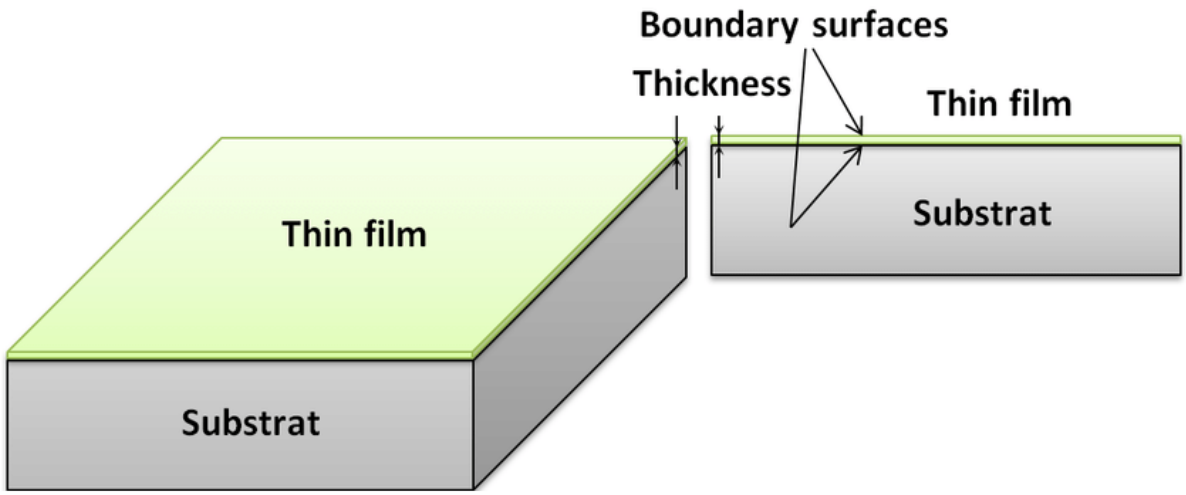

Figure II.1: *Schematic of thin film deposited on a substrate* [27].

II.2.1 Pulsed laser deposition (PLD)

- **Basics :**

Pulsed laser deposition (PLD) is the basic full slays of the position is physical vapor deposition (PVD) technique used to prepare thin films of a variety of materials. In this method, the target material is irradiated with a laser in short pulses, creating a plasma plume. Part of the extracted material is then deposited on the substrate, forming a thin film. The properties of the film depend on the deposition parameters such as the temperature, environment, pulse length, radiation intensity, deposition time, distance between the target and the substrate [28].

- **Mechanism :**

Electromagnetic radiation from a high intensity pulsed laser is used as an energy source to evaporate solid or liquid starting material which is called target, this laser is aimed at the target where the beam Interacts with surface and creates a luminous plasma plume , the plume itself consists of atoms molecules ions electrons however in same cases larger particulates and molten global of material can be ejected from the target during evaporation some of the extracted material is the deposited on the growth substrate forming a uniform film that has the desired composition structure roughness and thickness. the deposition process is carried out either in a vacuum or at a low gas

pressure environment which is achieved using vacuum pumps and vacuum gorges that are connected to the deposition chamber. ***Figure II.2*** [29].

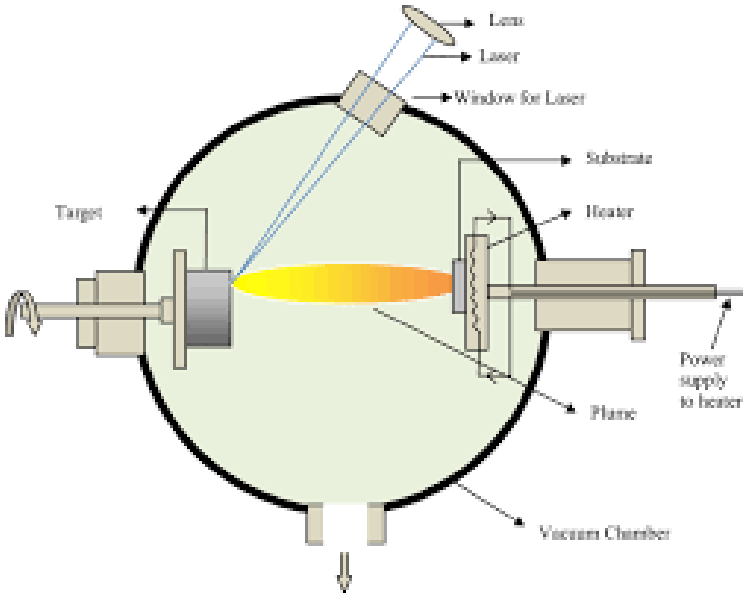

Figure II.2**:** *Schematic diagram of Pulsed Laser Deposition (PLD)* [30].

- **Properties :**

The most important properties of deposition films are the composition, crystallization roughness, thickness and other properties of the deposited film which depend on the parameters used to support the process, for example, the amount of material deposited by unit area is clearly dependent on the distance between the target and the substrate. The intensity wavelength and length of the laser pulses also have a significant effect on the excitation mechanism that takes place on target surface for instance using a laser with short pulses shorter than 1 picosecond electrostatic abolition occurs in which case the electrons that hold the material together are excited so fast that they leave the material resulting in an explosion of the small amount of target surface when nanosecond or longer laser pulses are used then the electronic excitations have time to relax and the energy is transferred to lattice vibrations of the target this is

causing a fast heating of the surface and evaporation of the target material which is called the thermal ablation mechanism if longer pulses are used then most of the impingement laser falls is absorbed by the plasma plume which further energizes the freshly created plasma . In either case the interaction of laser pulse and the target material results in highly energetic plasma plume which is directed away from the target surface it should also be noted that only a small amount of matter from the very top layer of the target is excited and extracted during each pulse this means that the deposition process is rather slow but on the other hand it also allows obtaining films that have a very high quality in addition this enables fine control over the thickness of the growing film .

The pulsed laser deposition process can be carried out in various gas environments at different pressures, which important because the pressure of the gas has a significant effect on the film growth rate crystallinity and stoichiometry , The deposition of metal oxides is normally carried out in the presence of oxygen to ensure that enough oxygen is bound on the metal surface and it should also be noted that the kinetic energy of the particles arriving on the growth substrate depends on the pressure of the gas in the chamber using background casts reduces the kinetic energy of the particles and allows obtaining fields with high crystallinity at lower pressures, The extracted particles are not slowed down and they hit the substrate with a higher energy this may cause localized damage and sputtering of the previously deposited film however when the gas pressure is too high then the energy of the atoms arriving on the growth substrate is not high enough to allow the formation of an ordered crystal structure the resulting film may be with low density and amorphous, Which in some cases maybe the targeted goal. The crystallinity of the ground films also depends strongly on the temperature of the substrate films deposited, at higher temperatures are normally crystalline while films made at lower temperatures rather amorphous. [29].

II.3 Characterization technique for deposited films

II.3.1 Electrical properties analysis

- **Four-point technique**

The four point probe technique is one of the most common methods for measuring resistivity and also used to measure sheet resistance of thin films, Particularly semiconductor thin films. Four-terminal sensing is used in some ohmmeters and impedance analyzers, and in wiring for strain gauges and resistance thermometers.

The four-point probe technique use to investigate how the measured resistance varies as a function of the position of the electrodes with respect to the edge of the sample. By using elementary electromagnetism concepts such as the superposition principle, the continuity equation, the relation between electric field and electric potential, and Ohm's law, There are two probes which are connected a current supply are placed outer side of all four point probes (1-4), And the other two probes measure the voltage between two probes. When the current is applied, the voltage change in read from the inner probes (2-3).The relationship between current and voltage is dependent to the resistivity of the thin films. As shown in ***Figure II.3***

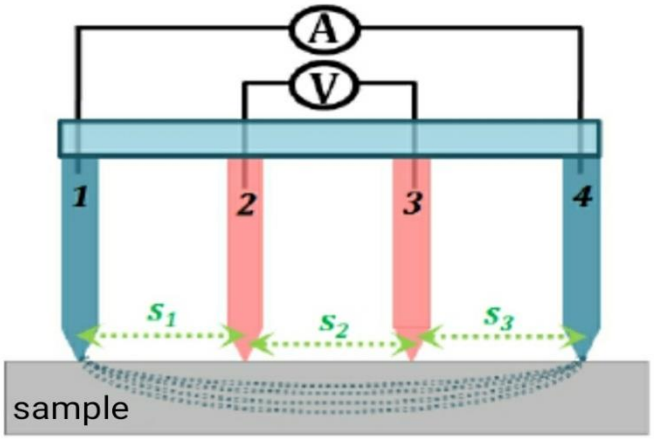

Figure II.3: *The structure of 4-point probe* [31].

The relationship between current through the outer probes and the voltage between the inner probes is dependent on the resistivity of the thin film. The resistivity is obtained by: the following ***Equation II.1***

$$\rho = (a\ 2\ \pi\ s)\ \mathrm{V}/I = 4.532\ t\ \mathrm{V}/I \qquad (\mathrm{II}.1)$$

Where (α) is a thickness correction factor which is plotted in ***Figure II.4*** below and t is the thickness of the thin film. Thin films we measure are in the range of t/s<<0.5, where a=0.72t/s.

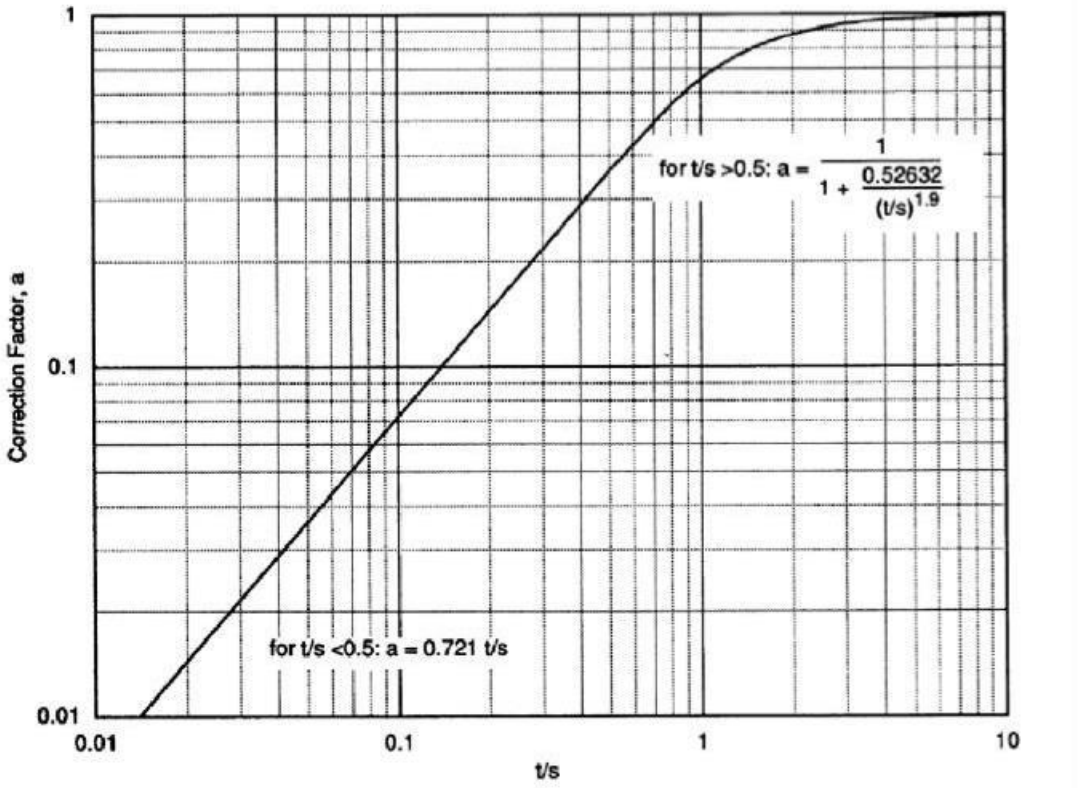

Figure II.4: *The thickness correction faction* [32].

If both sides of the **equation II.1** are divided by t we get the following ***Equation II.2***

$$Rs = \frac{\rho}{t} = 4.53\ \frac{\mathrm{V}}{I} \qquad (\mathrm{II}.2)$$

We refer to this as the sheet resistance, which has the units of ohms per square.

By using sheet resistances, we can calculate the TCR value of thin films by slowly varying the temperature with a substrate temperature controller. The value of TCR can be obtained by:

$$\alpha = \frac{1}{R}\ \frac{dR}{dT} \qquad (\mathrm{II}.3)$$

Where R is the sheet resistance of the thin film at the temperature T .We constructed a four point probe measurement system by purchasing the probe head from signatone, and building all the necessary translation stages and measurement equipment, as well as a substrate temperature controller .

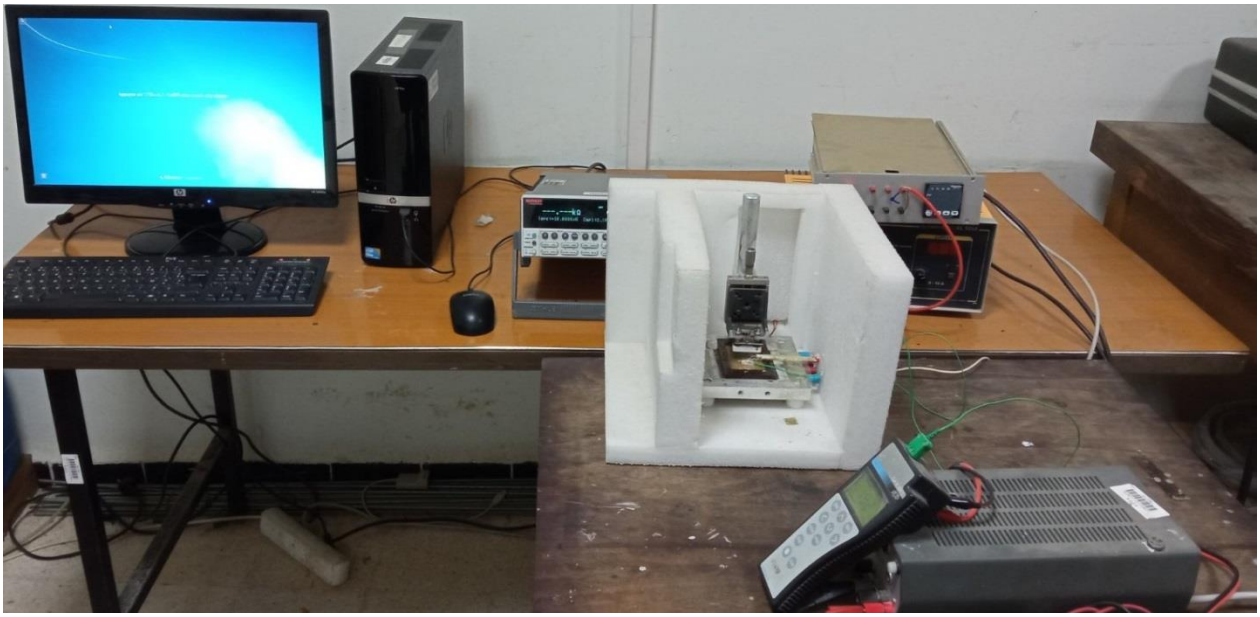

Figure II.5: *Photograph of the four-pointed device (CDTA)*.

- **Heating stage**

Heat treatments are combined operations of heating and cooling materials, in order to improve their characteristics and make them more favorable for a given use, Thermal cycle and based on two namely factors the temperature and time.

The objective of this heat treatment is to improve the physical properties of materials such as internal constraints, resistivity in addition to some chemical properties.

There are different types of heat treatments:

1. mass Processing : quenching, tempering, annealing
2. Surface treatments
3. Hardening by quenching after surface heating by electromagnetic induction, laser, plasma torch, plasma hexagon, electron beam.

In this study we are interested in annealing, witch is a heat treatment consists of heating the sample to a temperature above the point of transformation and then followed by long cooling after for the purpose of regenerating the sample or else removing the effect of the previous treatment and also an improvement in the mechanical properties and characteristics of the material and remove hardening (it is a plastic deformation which is sufficient after the manufacturing processes). ***Figure II.6***

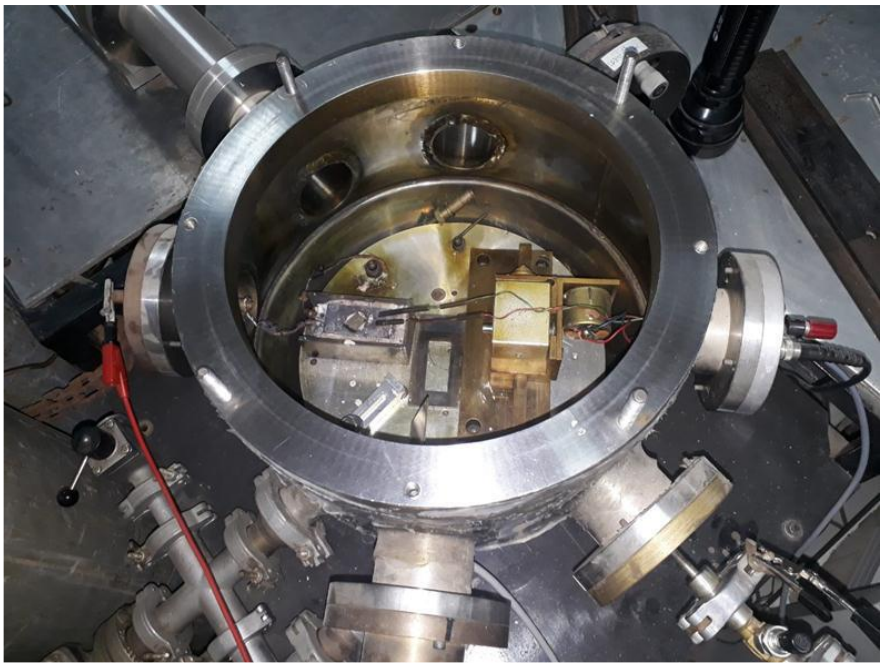

Figure II.6: *Photograph of the annealing device (CDTA).*

II.3.2 Structural analysis

- **X-ray diffraction (DRX)**

X-ray diffraction (XRD) is a nondestructive and highly quantitative technique which has been extensively used in the investigation of thin films [33]. It allows analyzing the crystallographic structure of matter.

X-ray diffraction (XRD) has several areas of using like reflectometry witch focused about the calculation of thickness; roughness and density. The grazing incidences are focused on the identification of the composition of the layer. And they have also powder diffraction that focus on the phase identification and crystallographic calculation.

The principle of the methods is based on the diffraction of X-rays by periodic atomic planes and the angle or energy-resolved detection of the diffracted signal. The geometrical interpretation of the XRD phenomenon (constructive interferences) has been given by W.L. Bragg. [34]. ***Figure II.7*** gives the details about the geometrical condition for diffraction and the determination of Bragg's law. Bragg's law is given in **Eq. II.4**

$$n\lambda = 2d\sin(\theta) \qquad (\text{II}.4)$$

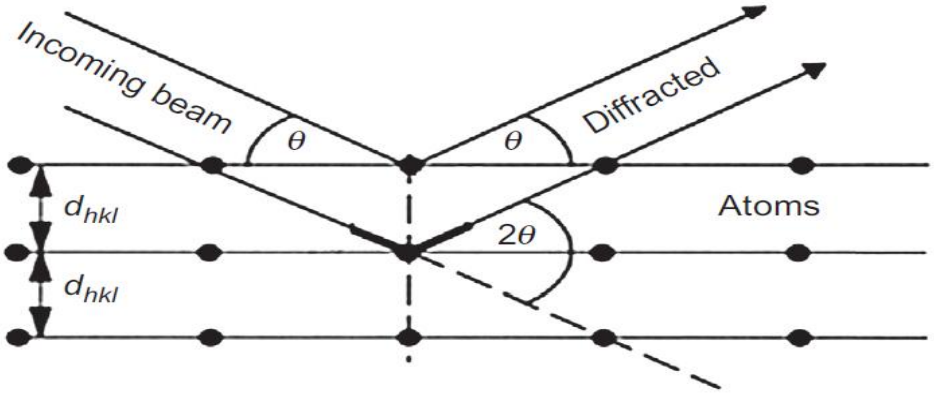

Figure II.7: *Geometrical condition for diffraction from lattice planes* [35].

Diffraction data are represented as intensity distribution as a function of the 2θ angle. The information content that can be extracted is represented in ***Figure II.8*** [36].

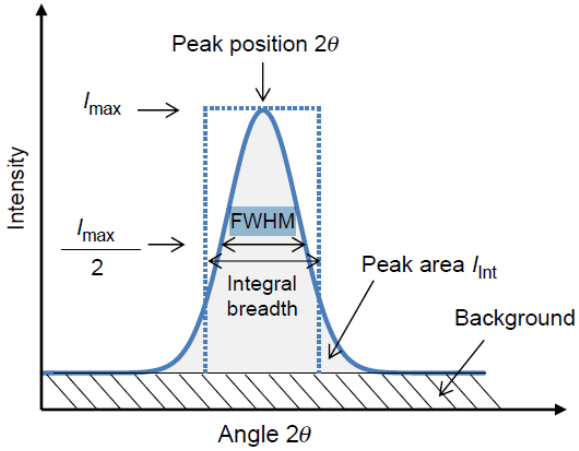

Figure II.8: *Diffraction peak and information content that can be extracted* [36].

In the case of thin films, the standard configuration (***Figure II.9-a***) gives much more structural information of the substrate than of the layer because the depth of penetration of the X-rays greatly exceeds the thickness of the layer (between 10 and 100µm) [37]. Using low angles of incidence under a configuration called grazing incidence X ray diffraction (***Figure II.9-b***), the path taken by X-rays in the layer can be significantly increased.

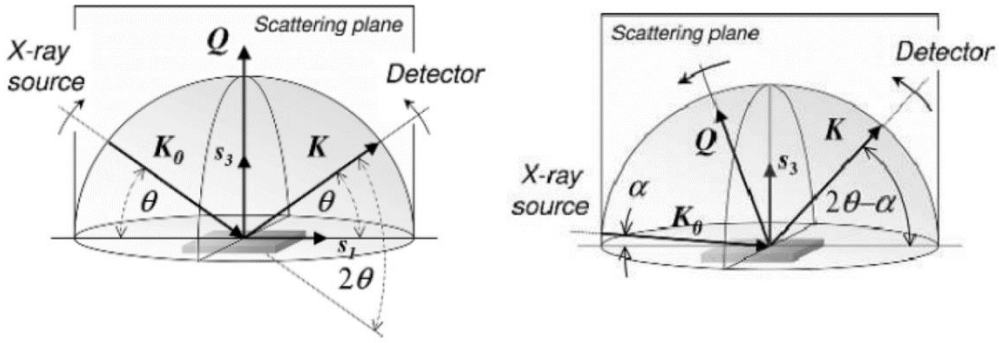

Figure II.9**:** *schematic representation of the symmetrical scan (a) in the standard configuration (b) asymmetric in the grazing configuration* [37].

The grazing incidence X-ray diffract meter will make it possible to carry out analyses of phases, crystalline texture and internal stresses on crystallized samples.
Structural characterization of massive samples or thin films at room temperature or at temperature according to different modes of analysis:

- θ / 2θ configuration or grazing incidence: Phase analysis, Crystal structure
- 4-circle configuration: Crystalline texture in layers of micron thickness
- 4-circle configuration with variable incidence: Determination of residual stresses ($\sin^2\varphi$ method), Analysis of diffraction line profiles (micro-deformation), Determination of the orientation of single crystals and internal co-stress of single crystals.

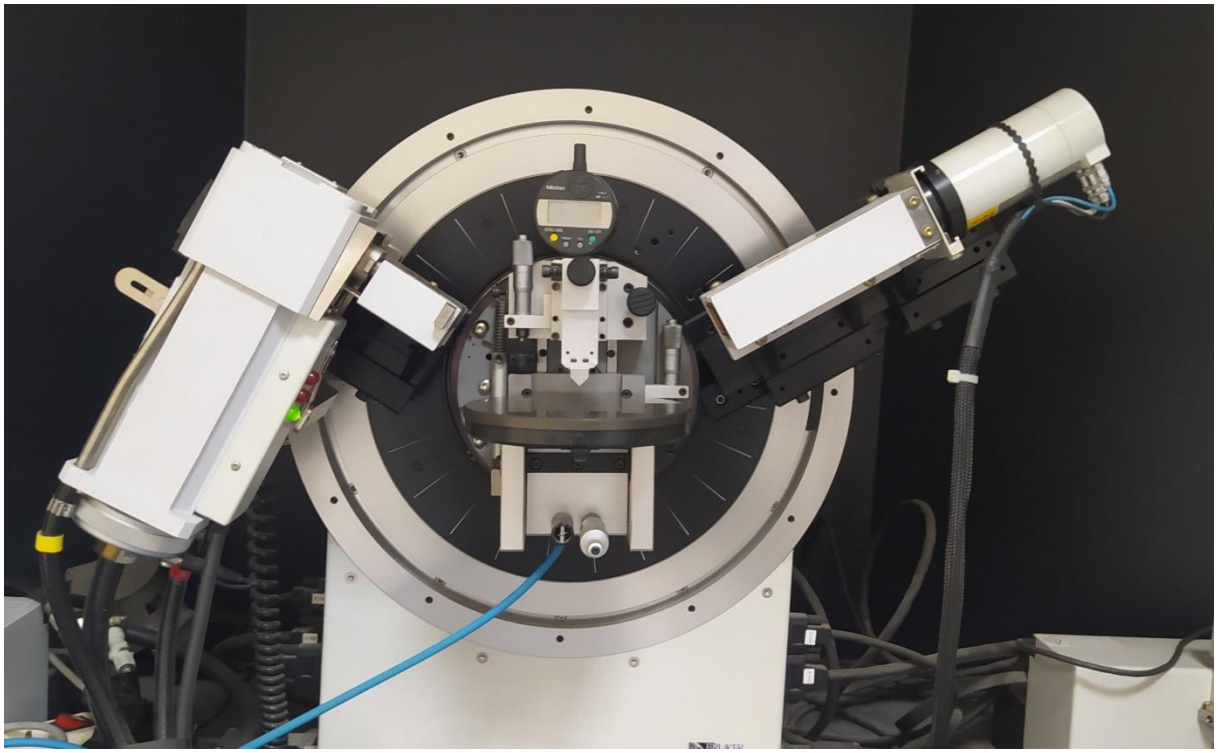

Figure II.10: *X-Ray diffraction (CDTA)*.

- **Raman spectroscopy :**

Raman is a light scattering technique, where by a molecule scatters incident light from a high intensity laser light source , typically in the infrared to UV wavelengths Of the incident photons, a few undergo Raman scattering, losing energy through exciting vibrational modes of the sample.

Of the incident photons, a few undergo Raman scattering, losing energy through exciting vibrational modes of the sample. These scattered photons are detected to make

a spectrum. Raman spectroscopy typically has a much larger depth of analysis compared to the other techniques [38]. **Figure II.11**

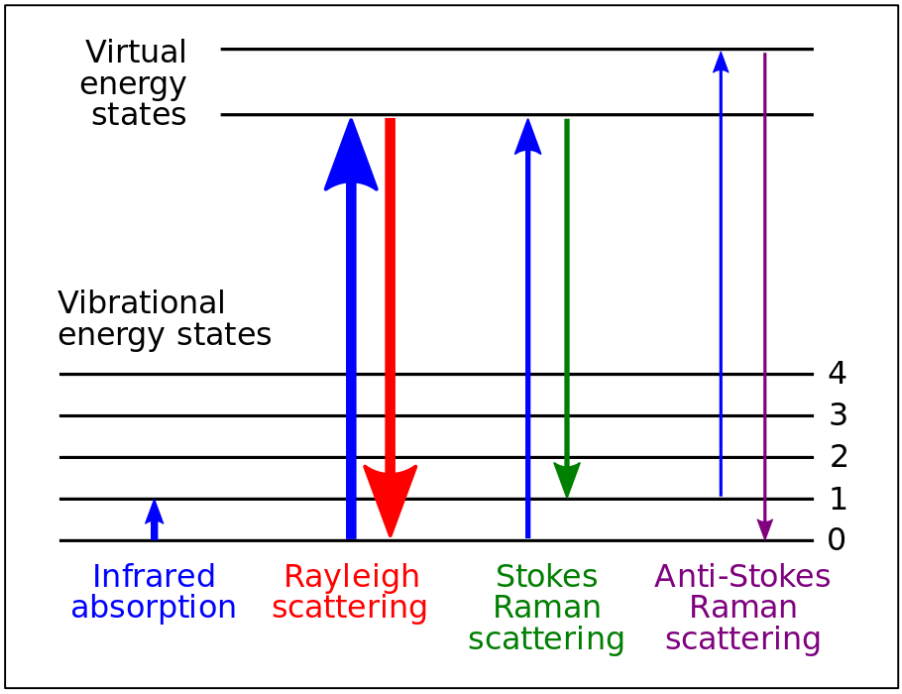

Figure II.11: *Diagram of the energy levels involved in infrared spectroscopy, Raman and Rayleigh scattering* [39].

A source of monochromatic light, usually from a laser in the visible, near infrared, or near ultraviolet range is used, although X-rays can also be used. The laser light interacts with molecular vibrations, phonons or other excitations in the system, resulting in the energy of the laser photons being shifted up or down. The shift in energy gives information about the vibrational modes in the system. Infrared spectroscopy typically yields similar yet complementary information.

Typically, a sample is illuminated with a laser beam. Electromagnetic radiation from the illuminated spot is collected with a lens and sent through a monochromatic. Elastic scattered radiation at the wavelength corresponding to the laser line (Rayleigh scattering) is filtered out by either a notch filter, edge pass filter, or a band pass filter, while the rest of the collected light is dispersed onto a detector [38]. **Figure II.12**

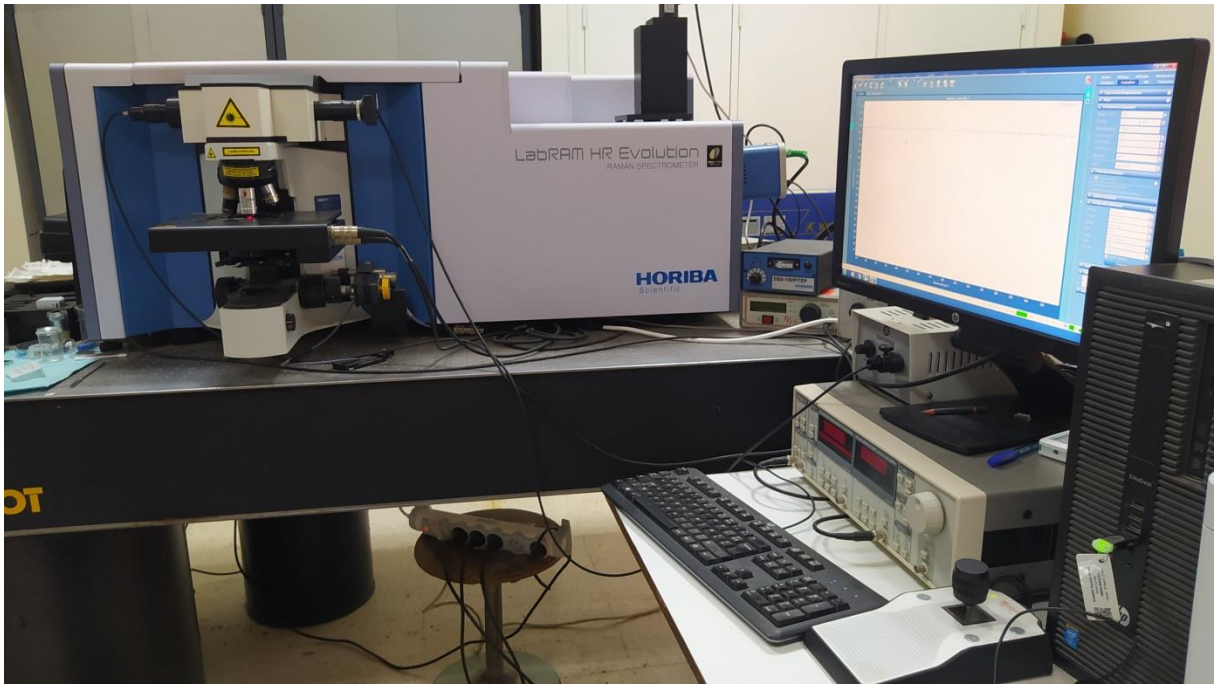

Figure II.12**:** *Raman spectroscopy device (CDTA)*.

Chapter III

Results and Discussion

Chapter III

III.1 Introduction

The main objective of this chapter is the study of the thermoresistive effect of vanadium pentoxide V2O5 and Zinc Oxide ZnO thin films were deposited on the substrates of glass characterized using the 4-point method and the heating stage, Then we analysis the structural with Raman spectroscopy and the XRD measurement. We aim to identify the electrical parameters, temperature coefficient of resistance (TCR) and resistivity, which control the active layers sensitivity for high-performance thermistor material.

III.2 Experimental details:

In this experimental we used two different metals oxides, V_2O_5 and ZnO at different thickness (1200nm, 500 nm and 100nm). Those thin films are synthesized by pulsed laser deposition technique with the parameters showing at the ***table III.1*** below:

V_2O_5	**PLD Parameters**	**ZnO**
1	**Laser fluency (Jcm^{-2})**	2
3	**Target-substrate distance (cm)**	4
300	**Temperature of the substrate (°C)**	300
10^{-2}	**Oxygen pressure (mbar)**	10^{-2}
200nm ⟶ 20 min	**Deposition time (min) And Thickness of thin film (nm)**	1200 nm ⟶ 26 min 500 nm ⟶ 15 min 100 nm ⟶ 03 min
5	**Laser frequency (Hz)**	5
Corning Glass	**Substrate used**	Corning Glass

Table III.1: *The PLD parameters of deposition for V_2O_5 and ZnO samples.*

The glass substrate was used for the advantages offering as it is an amorphous, insulating, transparent, and chemically inert solid material. From those properties, the glass as a substrate is convenient to determine the exact electrical properties of our samples.

III.3 Vanadium pentoxide V_2O_5

III.3.1 Structural analysis:

Figure III.1 Shows X-ray diffraction pattern of vanadium oxides films. A highly (001) oriented V_2O_5 was obtained according to JCPDS card N°: 892482.

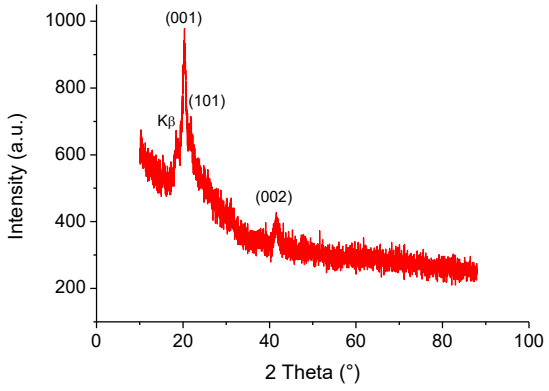

Figure III.1*: Grazing XRD of V_2O_5 thin film.*

The micro-Raman spectrum of PLD prepared VOx sample is shown in **Figure III.2.** V_2O_5 phase is clearly identified by its characteristic peaks at 145, 197, 283, 304, 405, 484; 529, 700 and 996 cm^{-1} [40]. Small peaks at 881 cm^{-1} and 937 cm^{-1} are observed. This shows the existence of a small amount of V_6O_{13} [41], which is not identified by XRD.

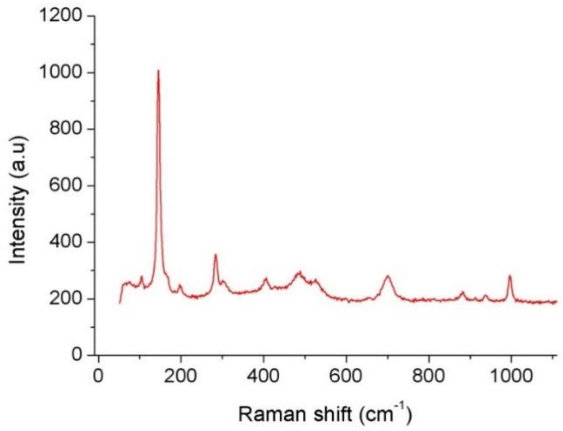

***Figure III.2**: Raman spectra of PLD vanadium pentoxideV_2O_5.*

III.3.2 Thermoelectrical measurements :

a) Study of temperature control :

The main objective of this study is to fix the input necessary power to reach 100°C. **First**, we study the variation of the temperature in function of time with different values of powers (10W, 15W, 18.7W, 20 W) without Thermo-regulator. See the **Figure III.3**

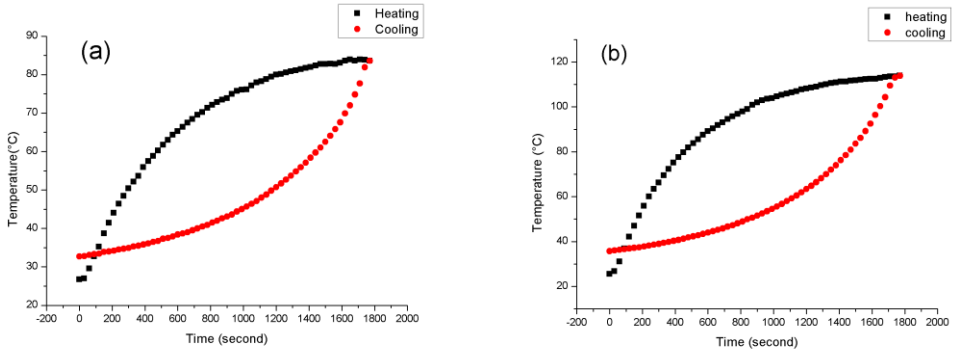

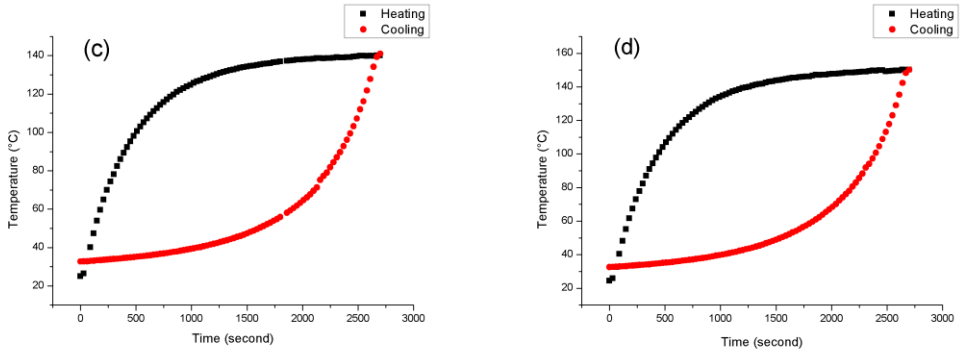

***Figure III.3**: Time dependence of the temperature at different powers: (a) 10W, (b) 15W, (c) 18.7W, (d) 20W.*

Second, From the later graphs, the maximum temperatures corresponding to each power and we obtain a linear relation between these last were plotted and are presented in **Figure III.4**.

Temperature (°C)	Power (W)
52,5	5
83,6	10
113,9	15
140,5	18,7
150,2	20

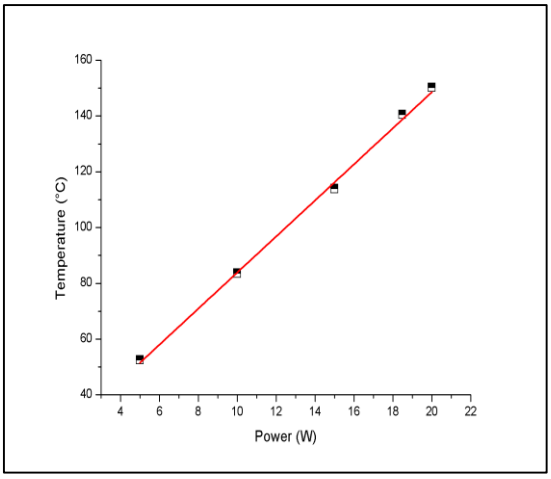

***Table III.2:** The maximum temperature temperature. for each power.*

***Figure III.4:** Power dependence of*

Finally, shows that 18 W is enough to realize our study because the thermal sensor they need to applicatied has a temperature range less than 100°C.

Here the input power of 18 W, we programmed the Thermo-regulator to increase the temperature with 2°C in every 1 min. This is really observed in **Figure III.5**

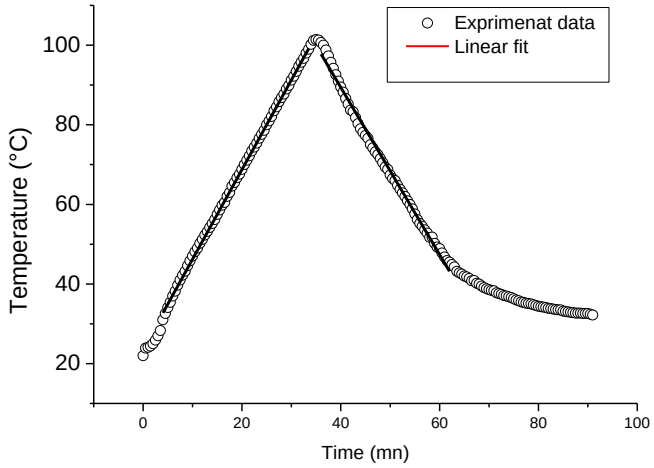

Figure III.5: *The Controlled-heating curve through the Thermo-regulator for 18 W input powers.*

b) Study of resistivity:

In this section we studied the effect of temperature on the electrical resistance, with the 4-point method.

1. Characteristics V-I :

At room temperature, an (I-V) measurement was set up for V_2O_5 sample chosen to confirm Ohm's law by confirming the linearity of the (I-V) graph shown in the **Figure III.6**.

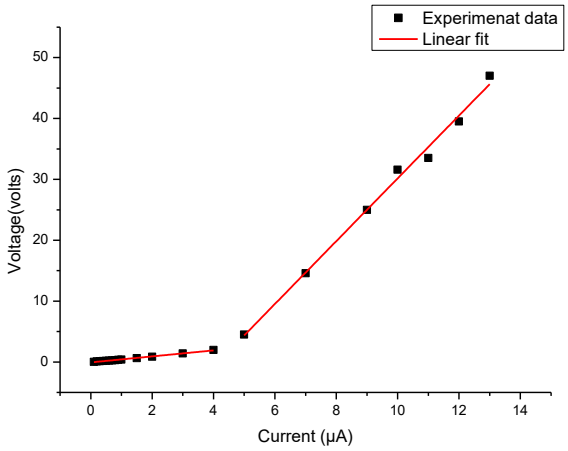

Figure III.6: *(V-I) Characteristics of V_2O_5 thin films.*

Figure III.6 Shows the V-I characteristics of V_2O_5 thin films. We observe a transition in the conductivity behavior at 5 μA bias current. So as bias currents, we choose 1μA from the first behavior and 10μA from the second.

The resistance measurement at room temperature:

First behavior from [0μA to 4μA]	R_1 =1.78 MΩ
Second behavior from [5μA to 13 μA]	R_2 =23.37 MΩ

TableIII.3:*V_2O_5 sample resistance.*

2. Temperature dependence on resistivity:

2.1: Bias at 1μA:

In this part, we will present the effect of temperature on electrical resistivity of V_2O_5 film, by fixing the current at 1μA. The voltage versus temperature is shown in the following graph:

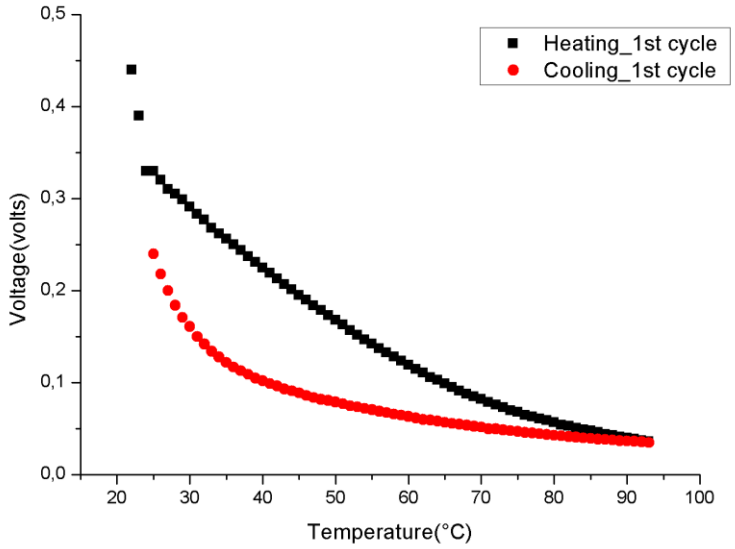

Figure III.7: *Voltage versus temperature plot for V_2O_5 thin film upon first thermal cycling.*

From **Figure III.7,** we notice the existence of a hysteresis, which is not suitable for practical use. In order to eliminate the hysteresis loop, multiples thermal cycling procedures has been performed as done in [42].

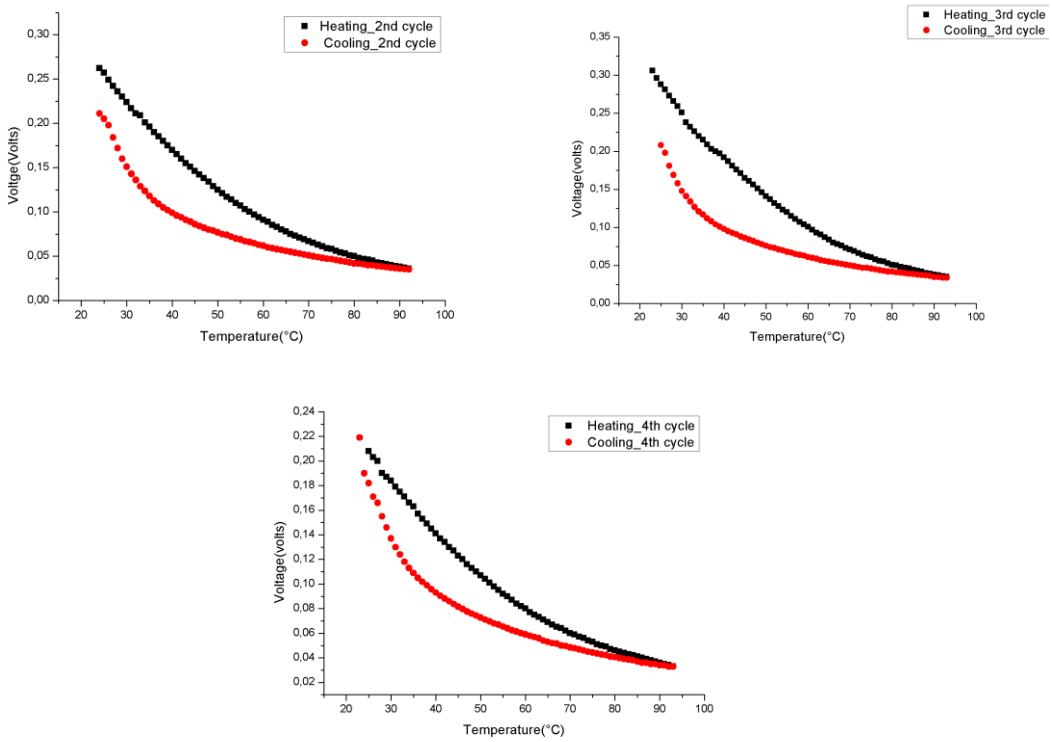

Figure III.8: *Voltage versus temperature plot for V_2O_5 thin film upon multiple thermal cycling.*

We notice that after 4 cycles we still obtained a hysteresis (see **Figure III.8**). Witch we think that is due to the presence in the film of small VO_2 Nano crystals as will proved below.

We reduced the temperature range for finding if we can take off the hysteresis; the first temperature range was from [0°C to 50°C] and the second was from [0°C to 40°C]. Effectively, according to **Figure III.9**, in the temperature range [0°C to 50°C], the hysteresis width is widely reduced, while in the [0°C to 40°C], the hysteresis loop is absent.

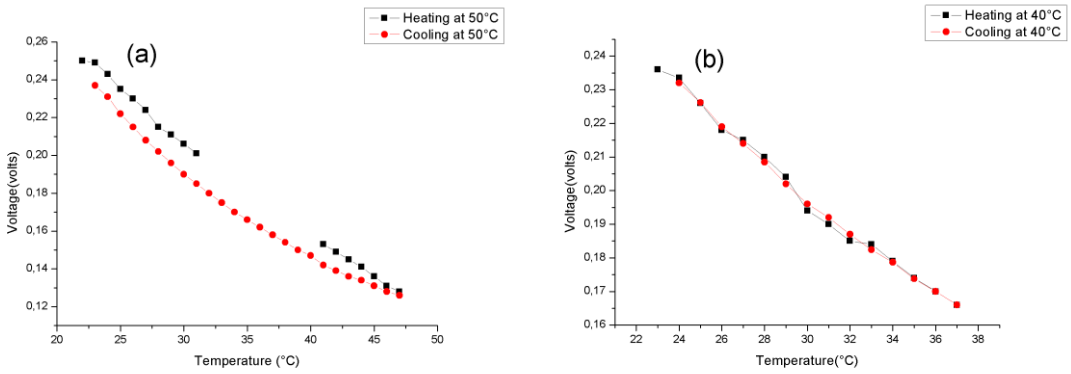

Figure III.9: *Voltage versus temperature plot for V2O5 thin films, (a)T= [0°C to 50°C], (b) T= [0°C to 40°C].*

2.2: Bias at 10µA:

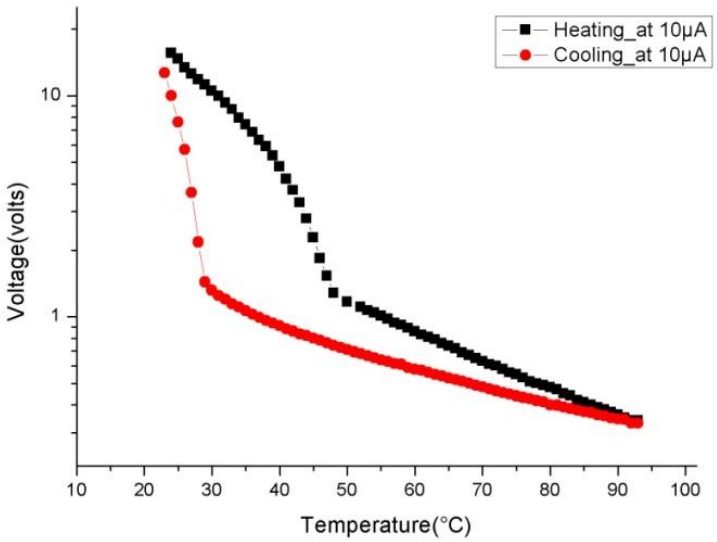

Figure III.10: *Voltage versus temperature plot forV_2O_5 thin film biased at 10 µA.*

We notice from **Figure III.10** a hysteresis loop that resembles to that of VO_2 compound. A relatively sharp drop and raise of the voltage can be observed at specific temperatures during, respectively, the heating and the cooling processes. To define precisely the transition temperature, we took the resistance log as versus of temperature, and then we fitted with a Gaussian function. The result is presented in **figure III.11**.

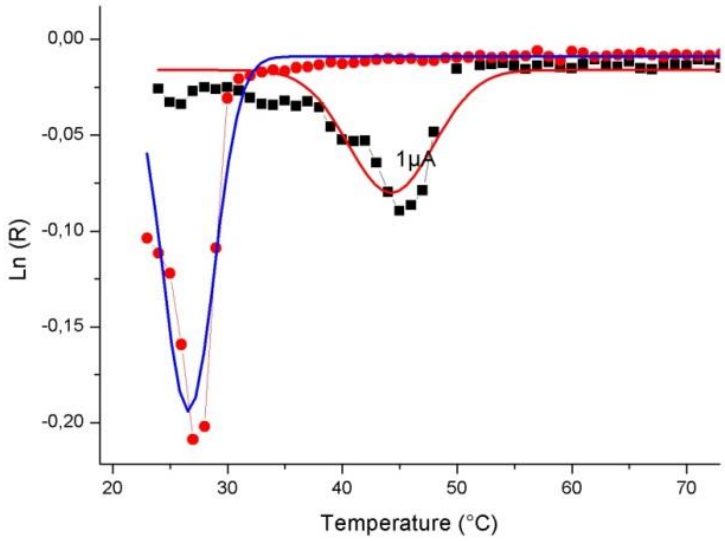

Figure III.11: *Transition curve.*

From **Figure III.11**, the insulator-metal-insulator transition temperatures are 45°C during heating and 27°C during cooling, which gives a hysteresis width of 18°C. Those transition characteristics are specific to nanocrystalline defectiveness VO_2 [43] .Also, we can define the initiation temperature for the transition to be ~ 37°C. This latter corresponds to the upper limit of the temperature range where the hysteresis loop was eliminated.

Resistivity measurement at room temperature:

We know that : $\boldsymbol{\rho = \varrho R}$

With ϱ it is the thickness of V_2O_5 thin layer. We given in table III.4

First behavior from [0µA to 4µA]	ρ_1 = 35.6 Ωcm
Second behavior from [5µA to 13 µA]	ρ_2 = 467.4 Ωcm

TableIII.4: *Results of resistivity in two behaviors for V_2O_5 sample.*

c) Temperature coefficient of resistance (TCR) measurement:

In this section, we highlight the dependence of the TCR to the bias current. First, we calculated TCRs in the temperature range where the hysteresis loop was absent, [0 to 37°C], for 1 and 10 µA bias currents. Second and for 10µA bias current, we calculated TCRs in the temperature range where the sharp drop of the voltage was observed, from the initiation temperature of the transition to the transition temperature, i.e. [37 to 47°C]

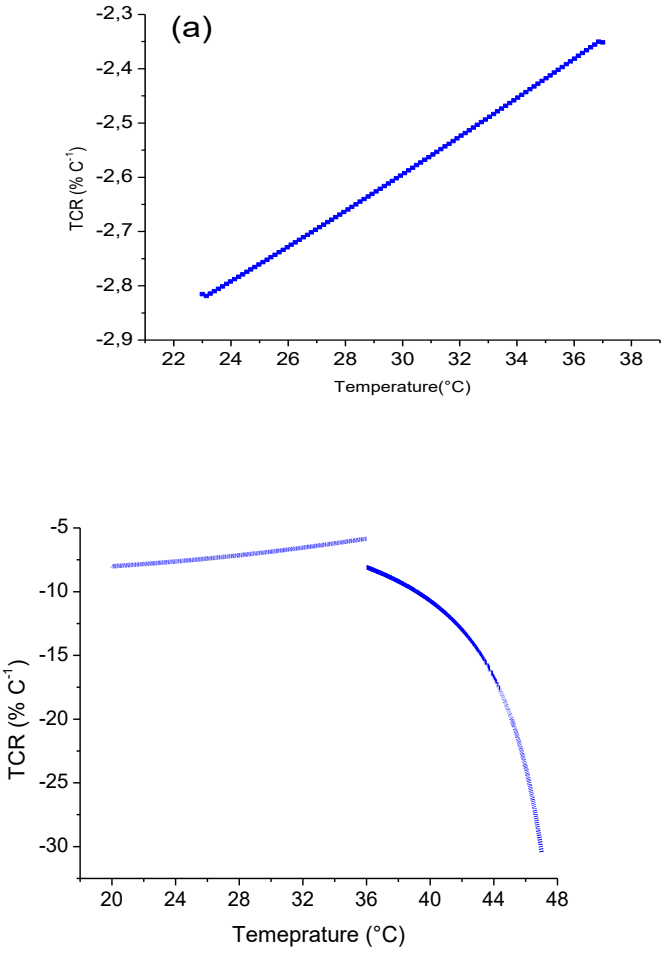

Figure III.12: *TCR versus temperature of V_2O_5 sample for bias current, (a) TCR at 1µA of bias,(b) TCR at 10µA of bias.*

FigureIII.12 (a) and (b) show that at room temperature (27°C), TCR is 2.7 % C and 7 % C , for respectively, 1µA and 10µA bias currents. For the last bias current, a huge TCR of 30 %C was obtained at 47°C corresponding to the transition temperature.

III.4 Zinc oxide ZnO:

III.4.1 Structural analysis:

Figure III.13 shows the XRD patterns of ZnO films deposited on glass as a function of film thickness. In all films, (002) peak, indexed to hexagonal wurtzite ZnO (JCPDS NO.36-1451), is the preferred orientation, independently of the thickness. The better crystallinity and highly intensity of preferential (002) orientation were obtained with thickness of 500 nm.

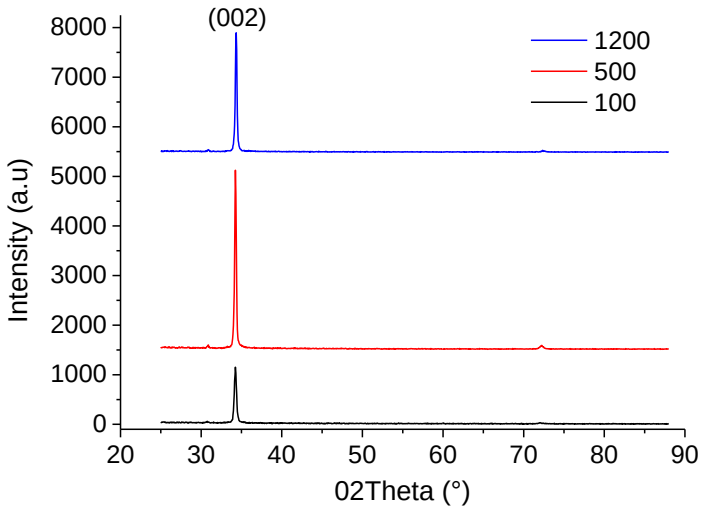

Figure III.13: *Grazing XRD patterns of ZnO thin films with different thickness.*

III.4.2 Thermoelectrical measurements:

Deposited zinc oxide thin films of different thickness were electrically characterized using 4 points method.

a) V-I Characteristics:

The V-I characteristics are presented in figure III-14.

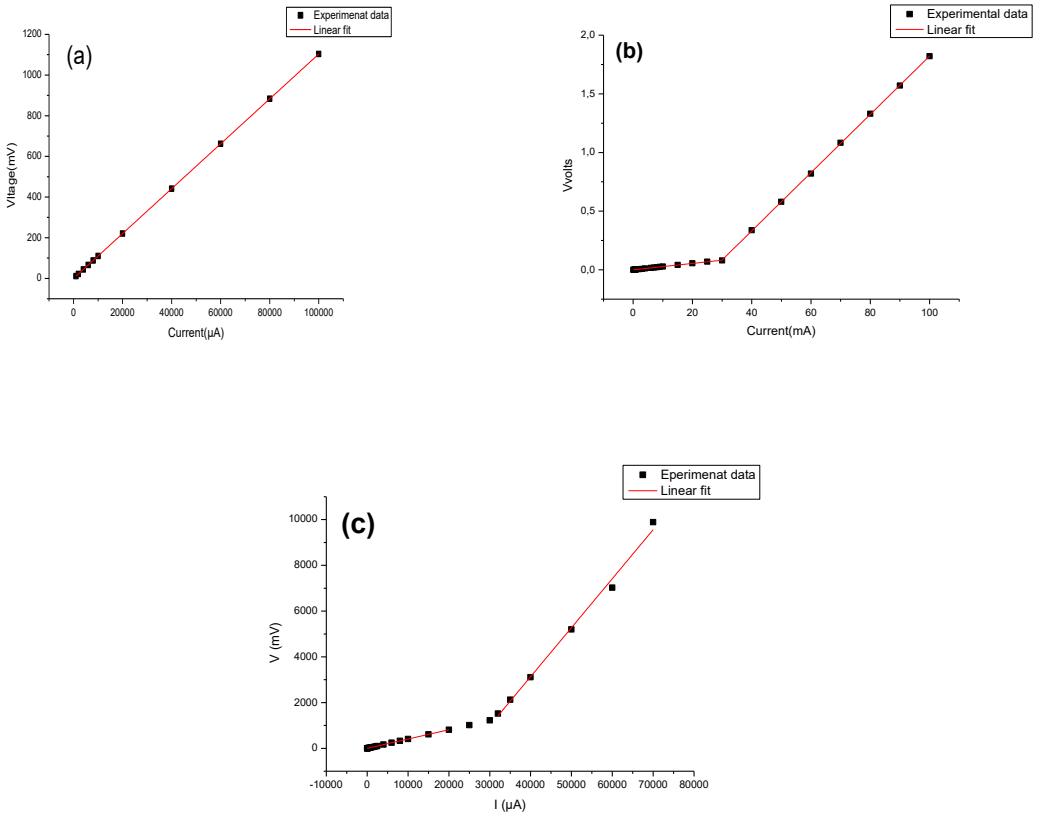

Figure III.14: *(V-I) Characteristics of ZnO thin films with different thickness, (a) 1200nm, (b) 100nm,(c) 500nm.*

Figure III.14 We obtained perfect ohmic behavior for ZnO with 1200nm of thickness however at ZnO 100nm we got two behaviors. The current threshold that caracterise the passage from the first to the second behavior is 30 mA. And finally the ZnO 500nm has also two behaviors with the same threshold current (30 mA).

The resistivity measurement:

	ZnO 1200nm	ZnO 100nm	ZnO 500nm
First behavior	R= 50 Ω $\rho = 6\ 10^{-3}$ Ωcm	R= 12 Ω $\rho = 1.2\ 10^{-4}$ Ωcm	R= 181 Ω $\rho = 9\ 10^{-3}$ Ωcm
Second behavior		R= 112 Ω $\rho = 10^{-3}$ Ωcm	R= 951 Ω $\rho = 5\ 10^{-2}$ Ωcm

TableIII.5: *Results of resistance-resistivity in different thickness of ZnO samples.*

b) Temperature dependence of resistivity :

1: Bias at 10mA of ZnO (1200nm)

In this part, we biased the current at 100mA than we measured the voltage versus temperature as showing in the graph below, see **Figure III.15**

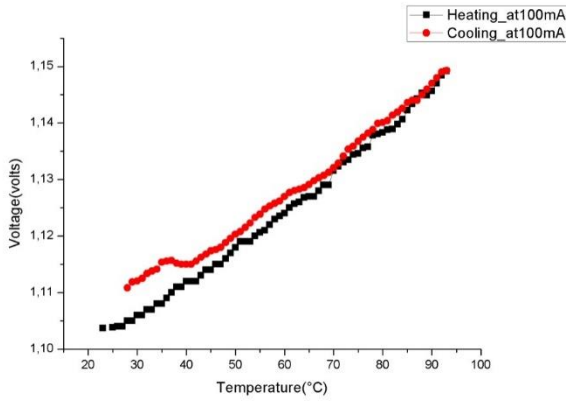

Figure III.15: *Voltage versus temperature plot for ZnO (1200nm) thin film.*

Figure III.15 Shows here that ZnO at 1200 nm thickness has a metallic behavior in function of temperature. This indicates that ZnO, here, is highly degenerated.

- **Temperature coefficient of resistance (TCR) measurement:**

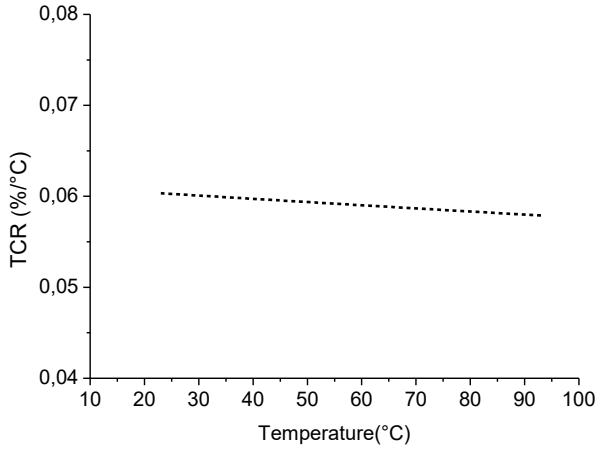

Figure III.16: *TCR of ZnO (1200nm) for bias current at 100mA.*

From **Figure III.16** we find a very low TCR = 0.06%/°C which is very stable along the used temperature range. This is typical for metals.

2: Bias at 10mA of ZnO (100nm):

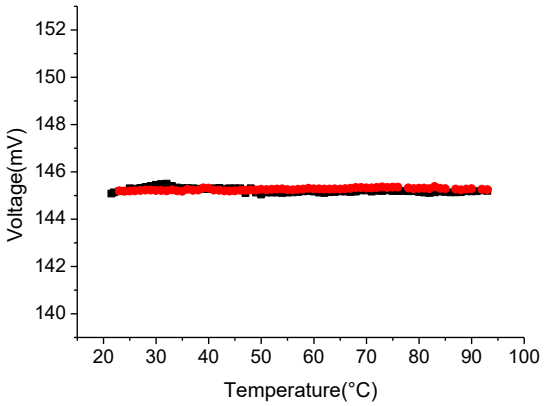

Figure III.17: *Voltage versus temperature plot for ZnO (100nm) thin film in different biased at 10 mA current.*

Figure III.17. Show that the resistivity doesn't depend on the temperature which means that TCR value is zero.

3: Bias at 100µA of ZnO (500nm):

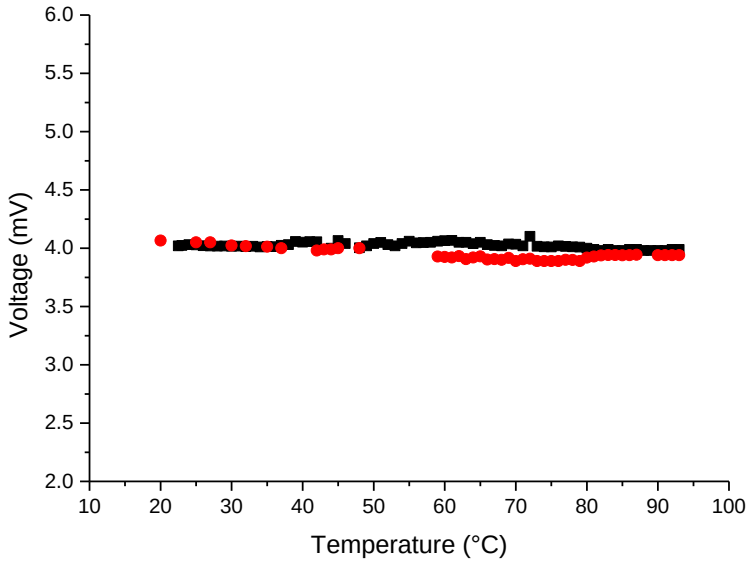

Figure III.18: *Voltage versus temperature plot for ZnO (500nm).*

From **Figure III.18** we obtain a constant voltage that is independent of temperature. We got again a TCR of zero as for 100 nm thickness.

In order to verify the thermal sensitivity of the 500 nm sample thickness throughout different values of the bias current, we have performed a V-I characteristics at a stabilized temperature of 90 °C. See **Figure III.19**

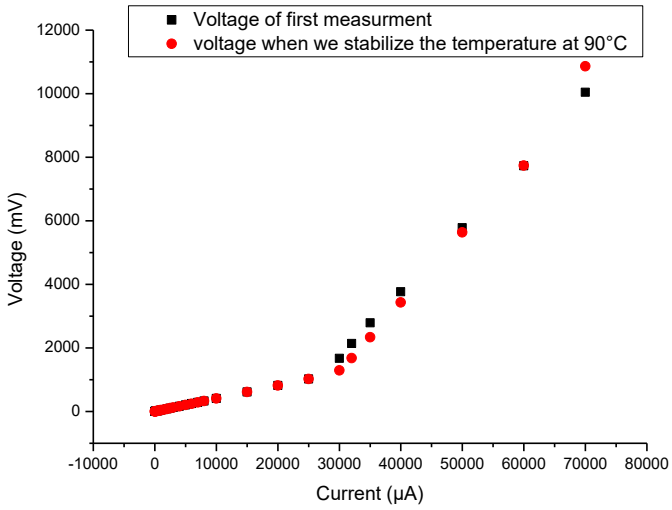

Figure III.19: *(V-I) Characteristics of ZnO 500nm after we stabilize the temperature at 90°*

Figure III.19 we confirmed that the sensitivity, i.e. TCR, of our sample is independent to the bias current. We notice here that TCR of zero value is desirable to design piezoresistive thin-film sensors [44].

Finally we notice that as our ZnO samples are highly degenerated due to specific PLD parameters used during the elaboration, mainly the oxygen pressure, the obtained TCR are not comparable to those generally reported (see chapter I).

Conclusion

CONCLUSION

The work presented in this work deals with the development and study of the properties of vanadium pentoxide and zinc oxide thin films, were we focused on the thermoelelectical measurements to study the thermal-resistive effect.

We have characterized the thin layers of vanadium pentoxide and zinc oxide by various methods: X-ray diffraction (XRD), Raman spectroscopy for structural study, and finally the method of the four points to determine the electrical properties of our layers. We particularly focused our attention on the effect of the temperature and the bias current.

A combined analysis through X-ray diffraction (XRD), Raman spectroscopy and electrical measurements are of great interest to analyze nanocomposite thin films. The analysis of vanadium oxide thin films shows a presence of V_2O_5 as a main phase with a mixture of V_6O_{13} and VO_2 phases.

The bias current and the heating temperature range control the TCR, the resistivity and the hysteresis loop. By using an appropriate bias current and at specific temperature range, the V_2O_5 thin films showed high TCR of 7%/° C at room temperature, non-desirable high resistivity (467 Ωcm) and absence of the hysteresis loop.

ZnO thin films are highly degenerated. The TCR is a thickness dependent. With very low resistivity in the range 10^{-2} to 10^{-4} Ωcm and a reversible behavior during heating and cooling cycles, near zero TCR was obtained for 100 and 500 nm thicknesses and a TCR of 0.06 %/°C was obtained for 1200 nm thickness.

Accordingly, due to the specific thermal-resistive properties of vanadium oxide nanocomposite thin films and ZnO thin films, vanadium oxide active layers are much more appropriate for thermal sensors and ZnO is appropriate for piezoresistive based sensors.

References:

[1] S. O. Kasap. (2006) Principles of Electronic Materials and Devices. NewYork,NY, USA: McGraw-Hil..

[2] S. M. Sze and K. K. Ng, Physics of Semiconductor Devices. Hoboken, NJ, USA: Wiley, 2006

[3] A. Feteira, “Negative temperature coefficient resistance (NTCR) ceramic thermistors: An industrial perspective,” J. Amer. Ceram. Soc., vol. 92, no. 5, pp. 967–983, 2009.

[4] N. T. Nguyen, “Micromachined flow sensors—A review,” Flow Meas. Instrum., vol. 8, no. 1, pp. 7–16, 1997.

[5] J. T. Kuo, L. Yu, and E. Meng, “Micromachined thermal flow sensors A review,” Micromachines, vol. 3, no. 3, pp. 550–573, 2012.

[6] J. Bahari, J. D. Jones, and A. M. Leung, “Sensitivity improvement of micromachined convective accelerometers,” J. Microelectromech. Syst., vol. 21, pp. 646–655, Jun. 2012.

[7] J. Bahari and A. M. Leung, “Micromachined three-axis thermal accelerometer with a single composite heater,” J. Micromech. Microeng., vol. 21, no. 7, p. 075025, 2011.

[8] Chandra Mohan Jha, (2015), Thermal Sensors Principles and Applications for Semiconductor Industries, DOI 10.1007/978-1-4939-2581-0.

[9] Zhang, J. X. J., & Hoshino, K. (2019). Mechanical transducers: Cantilevers, acoustic wave sensors, and thermal sensors. Molecular Sensors and Nanodevices, 311–412. doi:10.1016/b978-0-12-814862-4.00006-5.

[10] J. Vincent, G. Vampola, M. Pierce, Fundamentals of Infrared and VisibleDetector Operation and Testing, Wiley and Sons, 2015.

[11] Rajendra Kumar, R. T., Karunagaran, B., Mangalaraj, D., Narayandass, S. K., Manoravi, P., Joseph, M., & Gopal, V. (2003). Pulsed laser deposited vanadium oxide thin films for uncooled infrared detectors. Sensors and Actuators A: Physical, 107(1), 62–67. doi:10.1016/s0924-4247(03)00233-4.

[12] Hye Jin Lee, Dasom Wang, Tae Hyeong Kim, Dae-Han Jung, Tae-Hyeon Kil, Ki-Suk Lee, Hyung-Jin Choi, Seung-Hyub Baek, Euijoon Yoon, Won Jun Choi, Jeong Min Baik, Wide-temperature (up to 100 ◦C) operation of thermostable vanadium oxide based microbolometers with Ti/MgF_2 infrared absorbing layer for long wavelength infrared (LWIR) detection, Applied Surface Science 547 (2021) 149142.

[13] Shifeng Yu, Shuyu Wang, Ming Lu, and Lei Zuo, A metal-insulator transition study of VO_2 thin films grown on sapphire substrates, Journal Of Applied Physics 122, 235102 (2017).

[14] Chen, S., Lai, J., Dai, J., Ma, H., Wang, H., & Yi, X. (2009). Characterization of nanostructured VO_2 thin films grown by magnetron controlled sputtering deposition and post annealing method. Optics Express, 17(26), 24153. doi:10.1364/oe.17.024153.

[15] Bin Wang, Jianjun Lai, Hui Li, Haoming Hu, Sihai Chen, Nanostructured vanadium oxide thin film with high TCR at room temperature for microbolometer, Infrared Physics & Technology 57 (2013) 8–13.

[16] N. Fieldhouse, S. M. Pursel, R. Carey, M. W. Horn, and S. S. N. Bharadwaja, “Vanadium oxide thin films for bolometric applications deposited by reactive pulsed dc sputtering,” J. Vac. Sci. Technol. A 27(4), 951–955(2009).

[17] C. Venkatasubramanian, O. M. Cabarcos, D. L. Allara, M. W. Horn, and S. Ashok, “Correlation of temperature response and structure of annealed VO_x thin films for IR detector applications,” J. Vac. Sci. Technol. A 27(4), 956–961 (2009).

[18] C. Venkatasubramanian, M. W. Horn, and S. Ashok, “Ion implantation studies on VO_x films prepared by pulsed dc reactive sputtering,” Nucl. Instrum. Methods Phys. Res. B 267(8-9), 1476–1479 (2009).

[19] B. D. Gauntt, E. C. Dickey, and M. W. Horn, “Stoichiometry and microstructural effects on electrical conduction in pulsed dc sputtered vanadium oxide thin films,” J. Mater. Res. 24(4), 1590–1599 (2009).

[20] X.-F. Zhou, H. Zhang, Y. Li, X.-D. Tang, Q.-M. Chen, and P.-X. Zhang, Chin. Phys. Lett. 27, 018101 (2010).

[21] Battal, E.; Bolat, S.; Tanrikulu, M. Y.; Okyay, A. K. and Akin, T. Atomic-Layer-Deposited Zinc Oxide as Tunable Uncooled Infrared Microbolometer Material. Phys. Status Solidi A 2014, 211, 2475–2482.

[22] Zhou, X. Ag-Doping Improving The Detection Sensitivity Of Bolometer Based On ZnO Thin Films. Vacuum 2015, 117, 47-49.

[23] X.F. Zhou, H. Zhang, H. Yan, C.L. He, M.H. Lu, R.Y. Hao, Giant temperature coefficient of resistance in Co-doped ZnO thin films, Appl Phys A, DOI 10.1007/s00339-013-7665-8.

[24] N. Al-Khalli, M. Hezam, M. Alduraibi, M. Abdel-Rahman, Tuning of zinc oxide temperature sensing and optical absorption properties by tin heavy-doping, Materials Science in Semiconductor Processing 133 (2021) 105988.

[25] Sanchez, J. E., González, G., Vera-Reveles, G., Velazquez-Salazar, J. J., Bazan-Diaz, L., Gutiérrez-Hernández, J. M. González, F. J. (2017). Silver/zinc oxide self-assembled nanostructured bolometer. Infrared Physics & Technology, 81, 266–270. doi:10.1016/j.infrared.2017.01.019.

[26] H.J. Yuan, S.S. Xie, D.F. Liu ,X.Q. Yan, Z.P. Zhou, L.J. Ci, J.X. Wang, Y. Gao, L. Song, L.F. Liu, W.Y. Zhou, G. Wang, Characterization of zinc oxide crystal nanowires grown by thermal evaporation of ZnS powders, Chemical Physics Letters 371 (2003) 337–341.

[27] O.belahssen, Elaboration and characterization of thin-film gas sensor , El-Oued University, 2019.

[28] Robert Eason, Pulsed laser deposition of thin films applications-led growth of functional materials, 2007, Optoelectronics Research Centre University of Southampton, UK.

[29] H-U.Krebs, M.Weisheit, J.Faupel, E.Süske, T.Scharf, C.Fuhse, M.Stormer, K.Sturm, M.Seibt, H.Kijewski, D.Nelke, E.Panchenko, M.Buback, (2003). Pulsed Laser Deposition (PLD) -- A Versatile Thin Film Technique, Advances in Solid State Physics, 505–518, doi:10.1007/978-3-540-44838-9_36.

[30] https://image.app.goo.gl/2A9NpJABE5KRG1p59

[31] Arbenz Laure, Caractérisation des propriétés électromagnétiques des matériaux magnétiquement doux : application aux roues polaires de machine à griffes, l’École Nationale Supérieure d'Arts et Métiers, 2016.

[32] SP4 ordering info_2012, Lucas/Signatone Corporation

[33] Savaloni, H., Gholipour-Shahraki, M., & Player, M. A. (2006). A comparison of different methods for x-ray diffraction line broadening analysis of Ti and Ag UHV deposited thin films: nanostructural dependence on substrate temperature and film thickness. Journal of Physics D: Applied Physics, 39(10), 2231–2247. doi:10.1088/0022-3727/39/10/036.

[34] Bragg, W.L., 1913. The diffraction of short electromagnetic waves by a crystal. Proc Camb Philos Soc 17, 43e57.

[35] Spieß, L., Teichert, G., Schwarzer, R., Behnken, H., & Genzel, C. (2019). Moderne Röntgenbeugung. doi:10.1007/978-3-8348-8232-5.

[36] Epp, J. (2016). X-ray diffraction (XRD) techniques for materials characterization. Materials Characterization Using Nondestructive Evaluation (NDE) Methods, 81–124. doi:10.1016/b978-0-08-100040-3.00004-3.

[37] Birkholz, M. (2005). Thin Film Analysis by X-Ray Scattering. doi:10.1002/3527607595.

[38] D.J. Gardiner, P.R. Graves,Practical Raman Spectroscopy,Springer-VerlagBerlin Heidelberg. (1989), doi:10.1007/978-3-642-74040-4.

[39] https://image.app.goo.gl/EsBriDF15v2eWBfA7.

[40] Characterization of vanadium oxide thin films with different stoichiometry using Raman spectroscopy, Chunzi Zhang, Qiaoqin Yang, Cyril Koughia, Fan Ye, Mohsen Sanayei, Shi-JieWen, Safa Kasap, Thin Solid Films 620 (2016) 64–69).

[41] Characterization of vanadium oxide thin films with different stoichiometry using Raman spectroscopy, Chunzi Zhang, Qiaoqin Yang, Cyril Koughia, Fan Ye, Mohsen Sanayei, Shi-JieWen, Safa Kasap, Thin Solid Films 620 (2016) 64–69).

[42] THICKNESS EFFECT ON POST-ANNEALED VANADIUM OXIDE THIN FILMS DEPOSITED BY THERMAL EVAPORATION TECHNIQUE, Master, FERHI SANAA and BOUCHELAREM MANEL, Blida 1 university, 2020.

[43] R. Lopez, T. E. Haynes, L. A. Boatner, L. C. Feldman, R. F. Haglund, Jr. Phys. ReV. B 2002, 65, 224113.

[44] B.C. Marin, S. E. Root, A. D. Urbina, E. Aklile, R. Miller, A. V. Zaretski, D. J. Lipomi, ACS Omega 2017, 2, 626−630.